Alma Mater Studiorum · Università di Bologna

Scuola di Scienze
Corso di Laurea Magistrale in Fisica

Study of the calibration method of pressure-velocity probes and its application in a field of progressive plane waves

Supervisor:
Dott. Romano Zannoli

Correlator:
Dott. Domenico Stanzial

Presented by:
Fosca Fimiani

Session I
Academic Year 2015/2016

Abstract (English)

This dissertation presents a calibration procedure for a pressure velocity probe.

The dissertation is divided into four main chapters. The first chapter is divided into six main sections. In the firsts two, the wave equation in fluids and the velocity of sound in gases are calculated, the third section contains a general solution of the wave equation in the case of plane acoustic waves. Section four and five report the definition of the acoustic impedance and admittance, and the practical units the sound level is measured with, i.e. the decibel scale. Finally, the last section of the chapter is about the theory linked to the frequency analysis of a sound wave and includes the analysis of sound in bands and the discrete Fourier analysis, with the definition of some important functions.

The second chapter describes different reference field calibration procedures that are used to calibrate for the P-V probes between them the progressive plane wave method, which is that has been used in this work. Finally, the last section of the chapter contains a description of the working principles of the two transducers that have been used, with a focus on the velocity one.

The third chapter of the dissertation is devoted to the explanation of the calibration set up and the instruments used for the data acquisition and analysis. Since software routines were extremely important, this chapter includes a dedicated section on them and the proprietary routines most used are thoroughly explained. Finally, there is the description of the work that has been done, which is identified with three different phases, where the data acquired and the results obtained are presented. All the graphs and data reported were obtained through the Matlab® routine.

As for the last chapter, it briefly presents all the work that has been done as well as an excursus on a new probe and on the way the procedure implemented in this dissertation could be applied in the case of a general field.

Abstract (Italiano)

Il lavoro svolto in questi mesi ha permesso di definire una procedura di calibrazione per una sonda Pressione-Velocità.

La tesi è divisa in quattro capitoli principali. Il lavoro ha seguito la linea guida di un lavoro di ricerca riportato in [1].

Il primo capitolo è diviso in sei sezioni. Nelle prime due viene derivata l'equazione d'onda nei fluidi e la velocità del suono nei gas, la terza sezione tratta di una soluzione generale dell'equazione d'onda nel caso di onde piane. Nelle sezioni quattro e cinque viene riportata la definizione di impedenza e ammettenza acustiche, e le unità di misura pratiche attraverso cui è misurato il livello sonoro, i.e. la scala dei decibel. Infine l'ultima sezione del capitolo è relativa alla teoria legata all'analisi in frequenza di un'onda sonora. S'introduce l'analisi del suono in bande e l'analisi di Fourier, con la definizione di alcune funzioni importanti.

Il secondo capitolo descrive differenti procedure di calibrazione in un campo di riferimento, usate per calibrare le sonda P-V. Tre di queste sono riportate nella tesi tra cui il metodo di onda piana progressiva, usato in questo lavoro. L'ultima sezione del capitolo descrive i principi di funzionamento dei due trasduttori utilizzati focalizzandosi sulla descrizione del trasduttore di velocità.

La terza parte della tesi è dedicata alla spiegazione del set up di calibrazione e degli strumenti utilizzati per l'acquisizione e l'analisi dei dati. Data la centralità di alcune routine software utilizzate, vi è una loro descrizione in due sezioni dedicate, con un focus sulle routine proprietarie maggiormente utilizzate nell'analisi. Infine l'ultima sezione è dedicata alla descrizione del processo di acquisizione e analisi dei dati, suddividendo la fase operativa in tre fasi distinte ciascuna analizzata in una sottosezione dedicata. I grafici e dati riportati sono stati ottenuti tramite la routine di Matlab® scritta durante il lavoro il cui codice è riportato in appendice.

Infine nell'ultimo capitolo vengono riportate le conclusioni e alcuni sviluppi futuri del sensore.

Contents

Chapter 1

The Theory behind the Practice

1.1 The Wave Equation in Fluids

The only stress component in a fluid when viscous effects are assumed negligible is the hydrostatic pressure P. In the absence of wave motion, P has an equilibrium value P_e, which may vary with position, because of gravitational effects. When a compressional wave is passing through the fluid but the fluid is otherwise at rest, the local pressure differs from its equilibrium value by the amount [2]

$$p(\mathbf{r}, t) = P(\mathbf{r}, t) - P_e(\mathbf{r}). \tag{1.1.1}$$

We shall find it more convenient to use the incremental pressure p, rather than the total pressure P, as one of the dependent variables characterizing compressional waves in the fluid. The incremental pressure $p(\mathbf{r}, t)$ is a scalar function of position and time, whereas the related displacement of the fluid $\mathbf{d}(\mathbf{r}, t)$, if we define the displacement through the polar coordinates we have $\mathbf{d} = \xi\mathbf{i} + \eta\mathbf{j} + \zeta\mathbf{k}$ is a vector function of position and time. Since it is much easier to work with a scalar wave equation than with a vector equation, we regard p, rather than $\mathbf{d}$, as the basic dependent variable in the wave equation for compressional waves in the fluid. The volume strain, or dilatation D, which is associated with the incremental pressure, is related to the displacement $\mathbf{d}$ by the equation

$$D = \frac{\Delta V}{V} = \frac{\partial \xi}{\partial x} + \frac{\partial \eta}{\partial y} + \frac{\partial \zeta}{\partial z} = \nabla \cdot \mathbf{d}. \tag{1.1.2}$$

The incremental pressure and the accompanying dilatation are linearly related through the bulk modulus B

$$p = -BD = -B\nabla \cdot \mathbf{d}, \tag{1.1.3}$$

which express Hooke's law for fluid.

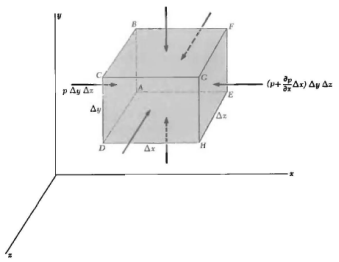

Figure 1.1.1: Forces acting on a fluid element.

Let us apply Newton's second law to the motion of the fluid contained in the cubical element $\Delta x\,\Delta y\,\Delta z$ shown in Fig. 1.1.1. As a first step, we need to find the net force on the element arising from wave-induced pressure variations on its six faces. The force in the x direction on the face ABCD is $p\,\Delta y\,\Delta z$, whereas the force in the x direction on the face EFGH is $[p + (\partial p/\partial x)\,\Delta x]\;\Delta y\,\Delta z$. Hence the net force in the positive x direction is

$$\Delta F_x = -\frac{\partial p}{\partial x}\Delta x\,\Delta y\,\Delta z. \tag{1.1.4}$$

Similarly the net forces in the positive y and z directions are

$$\Delta F_y = -\frac{\partial p}{\partial y}\Delta x\,\Delta y\,\Delta z \qquad \Delta F_z = -\frac{\partial p}{\partial z}\Delta x\,\Delta y\,\Delta z. \tag{1.1.5}$$

The net vector force on the cubical element is therefore

$$\Delta F = -\nabla p\,\Delta x\,\Delta y\,\Delta z,$$

where

$$\nabla p = \mathbf{i}\frac{\partial p}{\partial x} + \mathbf{j}\frac{\partial p}{\partial y} + \mathbf{k}\frac{\partial p}{\partial z} \tag{1.1.6}$$

is the pressure gradient. Since the vector acceleration of the fluid in the element is $\partial^2\mathbf{d}/\partial t^2$and its mass is $\rho_0\Delta x\,\Delta y\,\Delta z$, where ρ_0 is the density of the fluid, Newton's second law requires that

$$\Delta\mathbf{F} = -\nabla p\,\Delta x\,\Delta y\,\Delta z = \rho_0\Delta x\,\Delta y\,\Delta z\frac{\partial^2\mathbf{d}}{\partial t^2}. \tag{1.1.7}$$

On dividing through by $\Delta x\,\Delta y\,\Delta z$,

$$-\nabla p = \rho_0\frac{\partial^2\mathbf{d}}{\partial t^2}. \tag{1.1.8}$$

At this stage in deriving earlier wave equations, we expressed the elastic force, on the left side of the equations corresponding to (1.1.8), in terms of the appropriate strain component and elastic modulus. Since we now wish to regard the scalar pressure p, rather than the vector displacement $\mathbf{d}$, as the basic dependent variable, we need to use Hooke's law in the form (1.1.3) to eliminate $\mathbf{d}$

from the right side of (1.1.8). Let us therefore take the divergence of (1.1.8) to obtain an equation containing $\nabla \cdot \mathbf{d}$,

$$-\nabla \cdot \nabla p = \rho_0 \frac{\partial^2 (\nabla \cdot \mathbf{d})}{\partial t^2}. \tag{1.1.9}$$

By eliminating $\nabla \cdot \mathbf{d}$ using (1.1.3), we obtain the three-dimensional scalar wave equation

$$\nabla^2 p = \frac{1}{c_f^2} \frac{\partial^2 p}{\partial t^2} \tag{1.1.10}$$

where

$$c_f = \left(\frac{B}{\rho_0} \right)^{1/2} \tag{1.1.11}$$

is the wave velocity in the fluid, described more deeply in section 1.2. The left side of (1.1.9) is the three-dimensional Laplacian of the pressure p. In deciding to use the scalar wave equation (1.1.10) to describe compressional waves in fluids, we have not given up the possibility of finding the displacement $\mathbf{d}$ for a pressure wave that is the solution of (1.1.10). We need to compute the pressure gradient ∇p, substitute it in (1.1.8), and obtain the displacement in the wave by making two integrations with respect to time.

1.1.1 The Fluid Motion is Irrotational

In deciding to use the scalar wave equation (1.1.10) to describe compressional waves in fluids, we have not given up the possibility of finding the displacement e for a pressure wave that is the solution of (1.1.10). We need to compute the pressure gradient ∇p, substitute it in (1.1.8), and obtain the displacement in the wave by making two integrations with respect to time.

If the wave has a sinusoidal time dependence, the two integrations amount to dividing the expression being integrated by $-\omega^2$. Hence, for a sinusoidal wave of frequency ω,

$$d(\mathbf{r}, t) = \frac{1}{\rho_0 \omega^2} \nabla p_\omega(\mathbf{r}) e^{-i\omega t} \tag{1.1.12}$$

where $p_\omega(\mathbf{r})$ is the spatial part of the pressure wave. Evidently $p_\omega(\mathbf{r})$satisfies the time-independent wave equation

$$\nabla^2 p_\omega + \frac{\omega^2}{c_f^2} p_\omega = 0 \tag{1.1.13}$$

obtained by substituting

$$p(\mathbf{r}, t) = p_\omega(\mathbf{r}) e^{i\omega t} \tag{1.1.14}$$

in (1.1.10). Equation (1.1.13) is known as the scalar Helmholtz equation.

Equation (1.1.12) has an interesting consequence for wave motion in a fluid. We can easily show that the curl of the gradient of any scalar function of position is identically zero. Hence for

a compressional wave in a fluid satisfying (1.1.10) and having a sinusoidal time dependence the curl of the displacement vector vanishes, that is,

$$\nabla \times \mathbf{d} = 0 \tag{1.1.15}$$

Accordingly the strain accompanying such a wave is free from rotation. A vector function of position whose curl vanishes in some region is said to be irrotational in that region. By superposing many waves having the form of (1.1.12), it is possible to construct three-dimensional waves having a great variety of forms. All of these waves thus have the property of being irrotational.

1.2 The Sound Speed in Gases

Let us examine some of the consequences of the expression (1.1.11) for the velocity of compressional waves in a fluid before discussing solutions of the three-dimensional wave equation. It is usual to call the wave velocity in a fluid the velocity of sound.

A gas of molecular weight μ is a thermodynamic substance whose equilibrium state is determined by its pressure P and absolute temperature T. A definite volume V of the gas of mass m has the density $\rho_0 = m/V$ and contains $n = m/\mu$. moles. The so-called equation of state of the gas is a functional relation between P, V, and T for a specified amount of gas, such as 1 mole. Under equilibrium conditions, two of the state variables determine the third. The equation of state of real gases, for conditions remote from those causing liquefaction, is expressed to good approximation by that of an ideal gas

$$PV = nRT \tag{1.2.1}$$

where $R = 8,314 J/kg\,mole - deg$ is the universal gas constant, one of the fundamental constants of nature.

Thermodynamics teaches that we need to know more than the equation of state to specify completely the thermodynamic properties of a simple substance having the state variables P, V, and T. The additional information can consist of a knowledge of a specific heat, such as the specific heat at constant pressure C_p or the specific heat at constant volume C_v, as a function of temperature. With this information, and that of the equation of state, thermodynamics enables us to compute many other properties of the substance, including its bulk modulus B and therefore its velocity of sound.

Gases that have an equation of state closely approximated by (1.2.1) usually have nearly constant specific heats C_p and C_v over a limited temperature range. When such a gas is expanded (or compressed) in such a way that no heat flows into or out of the gas, a thermodynamic

calculation shows that the ideal gas then obeys the adiabatic equation

$$PV^{\gamma} = const \quad (adiabatic) \tag{1.2.2}$$

where $\gamma \equiv C_p/C_v$ is the (constant) ratio of the specific heats. When heat can flow so as to maintain constant temperature, the ideal gas obeys Boyle's law

$$PV = const \quad (isothermal). \tag{1.2.3}$$

Both these equations become more and more accurate for real gases in the limit of vanishing pressure.The corresponding sound velocities (1.1.11) are then

$$c_{ad} = \left(\gamma \frac{P}{\rho_0}\right)^{1/2} = \left(\gamma \frac{RT}{\mu}\right)^{1/2} = \left(\gamma \frac{kT}{m_0}\right)^{1/2} \tag{1.2.4}$$

$$c_{iso} = \left(\frac{P}{\rho_0}\right)^{1/2} = \left(\frac{RT}{\mu}\right)^{1/2} = \left(\frac{kT}{m_0}\right)^{1/2} \tag{1.2.5}$$

The final forms given in (1.2.4) and (1.2.5) express the velocities in microscopic (molecular) rather than macroscopic terms by substituting Boltzmann's constant $k = R/N$ and the mass of an individual molecule $m_0 = \mu/N$, where N is Avogadro's number.

The values obtained with the two methods give obviously different results and the one which is more similar to the experimental one is the velocity obtained through the adiabatic equation. As can clearly be seen in (1.2.4) the velocity of the air particles during the propagation of sound waves rely on the temperature of the air. Considering the sound velocity as reported in the formula above and replacing the following values $\rho_0 = 1,292\ kg/m^2$, $\gamma = 1,402$ at 0°C and $p_0 = 1\,atm = 1,0133 \times 10^5\,Pa$ the result is the value of sound velocity for an ideal gas:

$$c_{ad} = c_0 = \sqrt{1,402\left(\frac{1,0133 \times 10^5}{1,292}\right)} = 331,6\,m/s \tag{1.2.6}$$

which is really similar to the universal accepted value of $331,45\,m/s$ in the conditions stated above. As can be seen the velocity doesn't depend on the pressure as far as pressure and density compensate each other. The velocity depend strongly on temperature, $PV = nRT \rightarrow P = \rho MRT$ and so:

$$c_f = c_0\sqrt{\frac{T_{Kelvin}}{273,16}} = c_0\sqrt{1 + \frac{T_{celsius}}{273,16}}\ \ m/s. \tag{1.2.7}$$

1.3 General Solution of the Wave Equation

We now investigate the solutions of the wave equation (1.1.10) representing plane waves of sound in a uniform gaseous medium. Sound waves of this character can be obtained by moving a piston at one end of a long tube which could be considered as an ideal waveguide for plane compressional waves of sound whose wavelength is much greater than the lateral dimensions of the tube.

Let x be measured in the direction perpendicular to the plane wavefronts, so that the pressure in the sound wave is a function of x and t but not of y and z. The wave equation (1.1.10) then simplifies to

$$\frac{\partial^2 p}{\partial x^2} = \frac{1}{c^2}\frac{\partial^2 p}{\partial t^2} \tag{1.3.1}$$

and the general solution is

$$p = f\left(t - \frac{x}{c}\right) + g\left(t + \frac{x}{c}\right) \tag{1.3.2}$$

, if only the positive wave is considered the g term could be set equal to zero. The solution if the wave is a monochromatic sinusoidal is the following:

$$p = f\left(t - \frac{x}{c}\right). \tag{1.3.3}$$

1.3.1 Traveling Monochromatic Plane Waves

The pressure in a sinusoidal sound wave of frequency ω traveling in the positive x direction has the form[2]

$$p(x,t) = Pe^{i(kx-\omega t)} \tag{1.3.4}$$

where P is the real amplitude of the wave, and $k = 2\pi f$, from these quantities we also obtain $T = \frac{1}{f}\ [s]$ the period and $\lambda = 2\pi\frac{c}{\omega} = \frac{c}{f} = cT\ [m]$ the wave length. The usage of $k$and ω instead of f and λ is due to the fact we are dealing with functions, cosine and sine, which need angular arguments.

To find the displacement in the wave, we substitute the pressure gradient

$$\nabla p = \mathbf{i}\frac{\partial p}{\partial x} = \mathbf{i}ikPe^{i(kx-\omega t)} \tag{1.3.5}$$

in (1.1.12), which gives, after recalling that $k = \omega/c$

$$\mathbf{d}(x,t) = \mathbf{i}\xi(x,t) = \mathbf{i}\frac{i}{\omega\rho_0 c}Pe^{i(kx-\omega t)} \tag{1.3.6}$$

The displacement velocity in the wave is

$$\frac{\partial \mathbf{d}}{\partial t} = \mathbf{i}\frac{\partial \xi}{\partial t} = \mathbf{i}\frac{P}{\rho_0 c}e^{i(kx-\omega t)}. \tag{1.3.7}$$

From the comparison between the (1.3.4) and the (1.3.7), we find that the pressure and displacement velocity are in phase. The impedance of the wave is equal to ρc in each point x and in every single moment, t, it's used to define the specific impedance:

$$z = \frac{p}{\partial\xi/\partial t} = \rho_0 c = (B\rho_0)^{1/2} \tag{1.3.8}$$

is the characteristic wave impedance of the medium for plane sound waves, where the second term of the equality is the characteristic impedance of the medium.

The kinetic and potential energy densities in the wave are equal and depend on position and time in an identical manner, this is true in nondispersive media for all the traveling elastic waves we have investigated.

1.3.2 Standing Waves of Sound

If g in (1.2.2) is different from zero and we considered two traveling plane waves

$$\begin{aligned} p_1 &= \tfrac{1}{2} P e^{i(kx-\omega t)} \\ p_2 &= \tfrac{1}{2} P e^{i(-kx-\omega t)} \end{aligned}$$

occur simultaneously in a gaseous medium, thanks to the linearity property of the wave equation the combined wave

$$p = p_1 + p_2 = P cos\, kx\, e^{-i\omega t} \tag{1.3.9}$$

represents a one-dimensional standing wave. From (1.1.12) we find that the displacement in the wave is

$$\mathbf{d} = -\mathbf{i}\frac{P}{\omega\rho_0 c} sin\, kx\, e^{-i\omega t} \tag{1.3.10}$$

The standing wave is therefore given in real form by

$$\begin{aligned} p &= P cos\, kx\, cos\, \omega t \\ \mathbf{d} &= -\mathbf{i}\tfrac{P}{\omega\rho_0 c} sin\, kx\, cos\, \omega t \end{aligned} \tag{1.3.11}$$

The pressure and related displacement in the standing wave are out of phase with respect to position, but not with respect to time. A displacement node occurs at the origin and at positions spaced integral half-wavelengths from the origin. The pressure nodes symmetrically interlace the displacement nodes, so that a displacement (pressure) node occurs at a pressure (displacement) antinode.

Inside the impedance tube, standing wave propagate following the theory described above, it's interesting to calculate the impedance inside the tube which is one of the possible methods to calibrate the probe.

The impedance for a standing wave is given by the rate of the pressure in (1.3.10) and the derivative of the displacement in (1.3.11) which is:

$$\breve{Z}(0) = \rho_0 c \frac{\breve{Z}_l + j\rho_0 c \, tan \, kl}{\rho_0 c + j\breve{Z}_l \, tan \, kl} \tag{1.3.12}$$

where $j \equiv -i$.

This result directly relates the impedance load Z_l attached to the waveguide at$x = l$ to the input impedance of the waveguide which is a sinusoidal driving force applied at $x = 0$. Equation (1.3.12) tells us that $\breve{Z}(0)$ is a complex periodic function of the distance l separating the source and the load ends of the waveguide. Since the period of the tangent is π, $\breve{Z}(0)$ goes through a complete cycle of values when l covers the range of one-half wavelength. If, however, $\breve{Z}_l = \rho_0 c$, we find that $\breve{Z(0)} = \rho_0 c$, regardless of how long the waveguide is.

Suppose next that $\breve{Z}_l = 0$, indicating that the distant end is free, since a vanishing impedance permits a displacement velocity to exist with no accompanying force. The impedance at the source end is now a pure reactance,

$$\breve{Z}(0) = j\rho_0 c \, tan \, kl, \tag{1.3.13}$$

which can be made to have any value from $-j\,\infty$ to $+j\,\infty$ by choosing the value of l suitably[2].

1.4 Acoustic Impedance and Admittance

The term "impedance" has been coined from the verb 'impede' (obstruct, hinder), indicating that it is a measure of the opposition to the flow of current. The reciprocal of the impedance is the admittance usually defined as Y, $Y = Z^{-1} = G + iB$ coined from the verb 'admit' and indicating lack of such opposition [3].

There are many similarities between the equations describing the propagation of elastic waves in one dimension and the equations describing the propagation of waves of voltage and current on an electric transmission line.In electrical theory, the impedance of a linear circuit element having two terminals is the ratio of the complex sinusoidally varying voltage applied across the terminals to the complex current that flows in response to the voltage.

The electrical impedance Z is, in general, a frequency-dependent complex number, having a real part R and an imaginary part X. Its magnitude $(R^2 + X^2)^{1/2}$ gives the magnitude of the voltage-current ratio, and its phase angle $\phi = tan^{-1}(X/R)$ gives the phase angle between the voltage and current. If the linear circuit element is a pure resistance, then Z is simply the ohmic resistance R of the element.

The admittance, as already defined is $Y = G + iB$, where

$$G = \frac{R}{R^2 + X^2}$$

$$B = -\frac{X}{R^2 + X^2}.$$

As already stated in the acoustic case, when Z_c is real the (real) frequency-independent ratio has already been calculated in sec 1.3.1, and:

$$Z_c = \frac{p}{\partial\xi/\partial t} = \rho_0 c = (B\rho_0)^{1/2}$$

is the characteristic wave impedance of the medium for plane sound waves.

1.5 Practical Units for Measuring the Sound: the Decibel Scale

The human ear is able to perceive a difference in the pressure level from a minimum of $p_0 = 20\mu Pa$ to a maximum of $20\,Pa$, due to the wide variation range a logarithmic scale instead of a linear one has been chosen as the most appropriate, and so Decibel scale is logarithmic.

All the sound levels are expressed in dB and in this way it is possible to compare the sound level of pressure, velocity and intensity or obtain the sound level if just one of this quantities is defined.

1.5.1 Sound Pressure Level

The sound pressure in a point is the difference between the instantaneous pressure and the ambient mean pressure. The unit of Sound Pressure (p) is the Pascal (Pa) which is equal to one Newton per Square Meter (N/m^2). The reference value for Sound Pressure Level (SPL) is twenty micro-Pascal ($p_{ref} = 20\,\mu Pa$)[4]. The Sound Pressure Level (L_p) is defined by the following formula:

$$L_p = 20\,log\frac{p_{RMS}}{p_{ref}} \quad dB \tag{1.5.1}$$

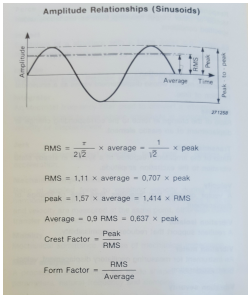

Figure 1.5.1: Definition of Root Mean Square (RMS).

where $p_{RMS} = lim_{T\to\infty}\frac{1}{2T}\int_{-T}^{T} p^2(t)dt$ which is equal to the Root Mean Square of a sinusoidal signal.

Sound Pressure and Sound Pressure Level refer to the Root Mean Square (RMS) value of the pressure. A pressure equal to the reference value is thus equal to zero dB while 1Pa equals 94 dB (93.98 dB). The zero dB value corresponds to the threshold of hearing at 1000Hz for a young

person with normal hearing ability.

1.5.2 Particle Velocity Level

The Air Particle Velocity, or just Particle Velocity ($\mathbf{v}$) is the velocity of a small volume of air (particle) in the neighborhood of the point where the pressure is evaluated. The dimensions of the volume regarded should be smaller in comparison with the wave-length but large with respect to intermolecular distances. The unit of particle velocity is meters per second (m/s). The particle velocity depends on the sound pressure and on the sound field conditions. Today, the recommended (ISO1683) reference for Particle Velocity Level (AVL - Average Velocity Level) is one nano-metre per second (1 nm/s or 10^{-9} m/s). However, fifty nano-metres per second ($50\,nm/s$) is also used, as this number was the commonly applied reference in the past, which is the value we use for this work to have the possibility to compare our results with the previous. The Particle Velocity Level (L_v) is defined by the formula below:

$$L_v = 20\,log\frac{\mathbf{v}}{v_{ref}} \quad dB \qquad where\ v_{ref}\ is\ 50\,nm/s \tag{1.5.2}$$

Particle Velocity and Particle Velocity Level generally refer to the Root Mean Square (RMS) value of the velocity signal, as defined before. This is considered if no reference is stated specifically. In the propagation direction of a plane progressive sound wave, the velocity level is approximately equal to the pressure level, if 50 nm/s is applied (to obtain a 94 dB level, the velocity needs to have a value of 2.5 mm/s, to obtain 120 dB, instead the velocity would be 5 cm/s). This is valid for normal ambient conditions i.e. for a static pressure of 101.325 kPa, a temperature of 23°C and for 50% Relative Humidity [4].

In this work, in order to have similar numerical values for both pressure and acoustic velocity, the following unit of measure, already defined in [5], is introduced

$$1Pa* = v\left[\frac{m}{s}\right] \cdot \rho_0 c \tag{1.5.3}$$

this is really useful because the pressure signal is expressed in Pa while the velocity one in m/s and they couldn't be compared, but the formula above there is the possibility to do it. It is really useful when talking about signal sensitivity, the value that multiplied for the signal returns the corrected one, so eq (1.5.3) allows to modify the units of the velocity signal from $V/(m/s)$ to $mV/Pa*$dividing the $V/(m/s)$ value for $((343 \cdot 1.2)/1000)$, an example:12.5 $[V/(m/s)] = 30.4\ [mV/Pa*]$.

1.5.3 Sound Intensity Level

Sound Intensity is acoustic power per unit of area. The unit of sound intensity is Watts per square-metre (W/m^2). The reference value for sound intensity is one pico-Watt per square-metre

($10^{-12} W/m^2$). The Sound Intensity Level is specified by the following formula (1.5.4):

$$L_I = 10\, log \frac{I}{I_{ref}} \quad dB \qquad where\ I_{ref}\ is\ 10^{-12}\ W/m^2 \tag{1.5.4}$$

In the propagation direction of a plane progressive sound wave, the sound intensity level is practically equal to the pressure level. The reference intensity is given by $I_{ref} = p_{ref} \cdot v_{ref} = 20 \cdot 10^{-6} \cdot\ 5 \cdot 10^{-8}$.

1.6 Frequency Analysis

The analysis of a waveform into its spectral components by the direct Fourier transformation (1.6.1) and the converse syndissertation of a waveform from its spectral components by the inverse Fourier transformation (1.6.2) lead to a systematic method for treating many cases of wave propagation in which the waveform is not sinusoidal. The method is applicable whenever the differential equations describing a physical system are linear, so that the principle of superposition is valid.

$$f(t) = \frac{1}{2\pi} \int_{-\infty}^{\infty} F(\omega) e^{-i\omega t} d\omega \tag{1.6.1}$$

$$F(\omega) = \int_{-\infty}^{\infty} f(t) e^{i\omega t} dt \tag{1.6.2}$$

The Fourier transform method is basically a technique for constructing a solution (a time-varying solution as described here) of a differential equation (or a system of differential equations). It is possible to use the Fourier transform method to construct a solution that has a specified dependence on time at a particular position, and considering also the spatial boundary through the spatial coordinate. The transform method deals most easily with a single independent variable, such as the time t.

Considering a linear physical system, which for simplicity we assume to depend for a fixed position in space, we would like to investigate its time varying properties.

If the system under discussion is excited in some particular manner at a particular position or boundary (position 1) by an external source which define the driving function, $p(t)$, the system responds, sooner or later with an output, effect, or response at some other position or boundary in the system (position 2): the response function or output, $q(t)$. Prior to the onset of the driving function we suppose that the system is quiescent.

It is important to note that the response $q(t)$ describes in a single expression both the transient[1] and the steady state response of the system. In table (1.6.1) some properties of the Fourier transform with the input-output pairs are reported, where $\breve{T}(\omega)$ is recognized as the transfer function of the system of stationary and progressive waves and $\breve{P}(\omega)$ is the Fourier inverse transform

[1] time before reaching the steady state, used also in recordings

of $p(t)$, through the (1.6.2).

	Driving function $p(t)$ at position 1	Response function $q(t)$ at position 2
Corollaries of linearity	$ap_1(t) \qquad a = cost$ $p_1(t) + p_2(t) + ...$	$aq_1(t)$ $q_1(t) + q_2(t) + ...$
Steady-state response to sinusoidal input	$e^{j\omega t}$	$\breve{T}(\omega)e^{j\omega t}$
Periodic function with a discrete spectrum	$\sum_{-\infty}^{\infty} \breve{P}(\omega_n)e^{i\omega_n t} \quad \omega_n = n\omega_1$	$\sum_{-\infty}^{\infty} \breve{P}(\omega_n)\breve{T}(\omega_n)e^{i\omega_n t}$
Non periodic function with a continuous spectrum	$\frac{1}{2\pi}\int_{-\infty}^{\infty} \breve{P}(\omega)e^{j\omega t}d\omega$	$\frac{1}{2\pi}\int_{-\infty}^{\infty} \breve{P}(\omega)\breve{T}(\omega)e^{j\omega t}d\omega$

Table 1.6.1: Fourier input-output pairs.

This is an elegant and efficient way of calculating the response $q(t)$ of a physical system to an arbitrary but known excitation function $p(t)$ provided that we know the transfer function $\breve{T}(\omega)$, i.e. the steady-state sinusoidal response (amplitude and phase) of the system as a function of frequency. The method assumes that the various definite integrals converge; these relations will be used during all the experimental work.

In our case $\breve{T}(\omega)$ is recognized as the wave impedance reported in the special case of stationary and progressive waves.

1.6.1 Frequency Band Analysis

Spectral analysis of a continuous signal is most commonly carried out in standardized frequency band analysis: octave and its fractions, for the analysis both analog and digital filters are available for this purpose. Such filters are referred to as constant percentage bandwidth filters meaning that the filter bandwidth is a constant percentage of the band center frequency. For example, the octave bandwidth is always about 70.1% of the band center frequency, the one-third octave bandwidth is 23.2% of the band center frequency and the one-twelfth octave is 5.8% of the band center frequency, where the band center frequency is defined as the geometric mean of the upper and lower frequency bounds of the band.

The stated percentages are approximate, as a compromise has been adopted in defining the bands to simplify and to ensure repetition of the center band frequencies. The compromise that has been adopted is that the logarithms to the base ten of the one-third octave center band frequencies are tenth decade numbers.

Besides constant percentage bandwidth filters, instruments with constant frequency bandwidth filters are also available. However, these instruments have largely been replaced by fast Fourier transform (FFT), which is an efficient numerical implementation of equation (1.6.1) analyzers which give similar results in a fraction of the time and generally at a lower cost. When

a time-varying signal is filtered using either a constant percentage bandwidth or a constant frequency bandwidth filter, an r.m.s. amplitude signal is obtained, which is proportional to the sum of the total energy content of all frequencies included in the band. When discussing digital filters and their use, an important consideration is the filter response time, TR(s), which is the minimum time required for the filter output to reach steady state. The minimum time generally required is the inverse of the filter bandwidth, B (Hz). That is

$$BT_R = \left(\frac{B}{f}\right) \cdot (fT_R) = bn_R \approx 1.$$

where the center band frequency, f, the relative bandwidth, b, and the number of cycles, n_R , have been introduced. For example, for a one-third octave filter $b = 0.23$ and the number of cycles $n_R = 4.3$. Where the r.m.s. value of a filtered signal is required, it is necessary to determine the average value of the integrated squared output of the filtered signal over some prescribed period of time called the averaging time. The longer the averaging time, the more nearly constant will be the r.m.s. value of the filtered output [6].

In the subsection below two different types of bands are described, which will also be used during the work of acquisition.

1.6.1.1 Octave Bands

The audio spectrum from about 20 Hz to 20 kHz can be divided up approximatively into 11 octave bands. If we define the 7th octave band's center (cnt) frequency to be $f_7^{cnt} = 1000\,Hz$, then all lower center frequencies for octave bands can be defined from each other using the formula $f_{n-1}^{cnt} = f_n^{cnt}/2$. Conversely, all higher center frequencies for octave bands can be defined from each other using the formula$f_{n+1}^{cnt} = 2 \cdot f_n^{cnt}$. Then for each center frequency, the half-octave low (high) frequency for each octave band are (respectively) given by the formula $f_n^{low} = f_n^{cnt}/2^{1/2}$ and $f_n^{high} = 2^{1/2} \cdot f_n^{cnt}$.

1.6.1.2 One Third Octave Bands

The audio spectrum can be divided up approximatively into 31, 1/3-octave bands. If we set/define the 19th 1/3-octave band's center frequency to be $f_{19}^{cnt} = 1000\,Hz$, then all lower center frequencies for 1/3-octave bands can be defined from each other using the formula $f_{n-1}^{cnt} = f_n^{cnt}/2^{1/3}$. Conversely, all higher center frequencies for 1/3-octave bands can be defined from each other using the formula $f_{n+1}^{cnt} = 2^{1/3} \cdot f_n^{cnt}$. Then for each center frequency, the 1/6-octave low (high) frequency for each 1/3-octave band are (respectively) given by the formulae $f_n^{low} = f_n^{cnt}/2^{1/6}$ and $f_n^{high} = 2^{1/6} \cdot f_n^{cnt}$.

1.6.2 Discrete Fourier Transform (DFT) and Important Functions

As already stated in section 1.6.1 every function can be analyzed through the Fourier analysis which is the process of decomposition of a time-varying signal into a spectrum of its sinusoidal components, i.e, the transformation of a signal from the time domain to the frequency domain.

The form of Fourier transform pair used in spectrum analysis instrumentation is referred to as the discrete Fourier transform, for which the functions are sampled in both the time and frequency domains. Thus:

$$x(t_k) = \sum_{n=0}^{N-1} X(f_n) e^{j2\pi nk/N} \quad k = 1, 2, 3...N \tag{1.6.3}$$

$$X(f_n) = \frac{1}{N} \sum_{n=0}^{N-1} x(t_k) e^{-j2\pi nk/N} \quad n = 1, 2, 3...N \tag{1.6.4}$$

where k and n represent discrete sample numbers in the time and frequency domains, respectively[6].

1.6.2.1 Sampling Process

In signal processing, sampling is the reduction of a continuous signal to a discrete signal, DFT. A common example is the conversion of a sound wave (a continuous signal) to a sequence of samples (a discrete-time signal).

Sampling can be done for functions varying in space, time, or any other dimension, and similar results are obtained in two or more dimensions.

For functions that vary with time, the sampling is done every T seconds, which is called the sampling interval, the sampling frequency or sampling rate, f_s, is the average number of samples obtained in one second (samples per second), thus $f_s = 1/T$.

1.6.2.2 Power Spectrum

The Power Spectrum is the most common form of spectral representation used in acoustics and vibration. If the previous analysis is extended to the more general case of non-periodic (or random noise) signals by allowing the period, T, to become indefinitely large, than X_n becomes $X'(f)$: a continuous function of frequency, f. It is important to note here that whereas the units of X_n are the same as those of $x(t)$, the units of $X'(f)$ are those of $x(t)$ per Hertz, named spectral density function. With the proposed changes, Equation (1.6.4) takes the following form:

$$X'(f) = \int_{-\infty}^{\infty} x(t) e^{-j2\pi ft} dt. \tag{1.6.5}$$

where $j = -i$, reported in (1.6.2).

The spectral density function, $X'(f)$, is complex, characterized by a real and an imaginary part (or amplitude and phase): Equation (1.6.3) becomes:

$$x(t) = \int_{-\infty}^{\infty} X'(f) e^{j2\pi ft} dt. \tag{1.6.6}$$

The spectrum of squared amplitudes is known as the power spectrum:

$$\textit{power spectrum} = \int_{-\infty}^{\infty} |x(t)|^2 \, dt \quad \textit{and also to} \quad \textit{power spectrum} = \int_{-\infty}^{\infty} \left|X'(f)\right|^2 df \tag{1.6.7}$$

which leads to the Parsival Theorem: $\int_{-\infty}^{\infty} |x(t)|^2 = \int_{-\infty}^{\infty} |X'(f)|^2 \, df$.

For a finite record length, T, the two-sided power spectrum may be estimated using:

$$S_{xx}(f_n) = \frac{1}{q} \sum_{i=1}^{q} X_i^*(f_n) X_i(f_n) \tag{1.6.8}$$

where q is the number of spectra over which the average is taken and X^* indicates the complex conjugate of X. The larger the value of q, the more closely will the estimate of $S_{xx}(f_n)$ approach its true value. In practice, the two-sided power spectrum $S_{xx}(f_n)$ is expressed in terms of the one sided power spectrum $G_{xx}(f_n)$ where:

$$\begin{aligned} G_{xx}(f_n) &= 0 & f_n < 0 \\ G_{xx}(f_n) &= S_{xx}(f_n) & f_n = 0 \\ G_{xx}(f_n) &= 2S_{xx}(f_n) & f_n > 0 \end{aligned} \tag{1.6.9}$$

1.6.2.3 Cross-spectrum

The two-sided cross-spectrum between two signals $x(t)$ and $y(t)$ in the frequency domain can be defined as follows:

$$S_{xy}(f_n) = \frac{1}{q} \sum_{i=1}^{\infty} X_i^*(f) Y_i(f) \tag{1.6.10}$$

$X_i(f)$ and $Y_i(f)$ are the spectra and $S_{xy}(f_n)$ is the average of their product. In contrast to the power spectrum in (1.6.8) which is real, the cross-spectrum is complex, characterized by an amplitude and a phase. In practice, the amplitude of $S_{xy}(f_n)$ is the product of the two amplitudes $X(f_n)$ and $Y(f_n)$ and its phase is the difference in phase between $X(f_n)$ and $Y(f_n)$, $\theta_y - \theta_x$. This function can be averaged because for stationary signals, the relative phase between x and y is fixed and not random. The cross-spectrum S_{yx} has the same amplitude but opposite phase $(\theta_x - \theta_y)$ to S_{xy}.

As for power spectra, the two-sided cross-spectrum can be expressed in single-sided form as:

$$G_{xy}(f_n) = 2S_{xy}(f_n) \quad f_n > 0. \tag{1.6.11}$$

Note that $G_{xy}(f)$ is complex, with real and imaginary parts referred to as the cospectrum and quad-spectrum respectively. As for power spectra, the accuracy of the estimate of the cross-spectrum improves as the number of records over which the averages are taken increases. The statistical error for a stationary Gaussian random signal is given as:

$$\epsilon = \frac{1}{\sqrt{\gamma^2(f)q}} \tag{1.6.12}$$

where $\gamma^2(f)$ is the coherence function (see next section) and q is the number of averages.

1.6.2.4 Coherence

The coherence function is a measure of the degree of linear dependence between two signals, as a function of frequency. It is calculated from the two auto-spectra (or power spectra) and the cross-spectrum as follows:

$$\gamma^2(f) = \frac{|G_{xy}(f)|^2}{G_{xx}(f) \cdot G_{yy}(f)}. \tag{1.6.13}$$

By definition, $\gamma^2(f)$ varies between 0 and 1, with 1 indicating a high degree of linear dependence between the two signals, $x(t)$ and $y(t)$. Thus in a physical system where $y(t)$ is the output and $x(t)$ is the input signal, the coherence is a measure of the degree to which $y(t)$ is linearly related to $x(t)$. If random noise is present in either $x(t)$ or $y(t)$ then the value of the coherence will diminish. Other causes of a diminished coherence are a undamping relationship between $x(t)$ and $y(t)$, insufficient frequency resolution in the frequency spectrum or poor choice of window function. A further cause of diminished coherence is a time delay, of the same order as the length of the record, between $x(t)$ and $y(t)$.

The main application of the coherence function is in checking the validity of frequency response measurements. Another more direct application is the calculation of the signal, S, to noise, N, ratio as a function of frequency:

$$S/N = \frac{\gamma^2(f)}{1 - \gamma^2(f)}. \tag{1.6.14}$$

1.6.2.5 Transfer Function

The transfer function $H(f)$ is defined as:

$$H(f) = \frac{Y(f)}{X(f)}. \tag{1.6.15}$$

Note that the frequency response function $H(f)$ is the Fourier transform of the system impulse response function, $h(t)$, $Y(f)$ is the frequency transform of $y(t)$ and $X(f)$ is the frequency transform of $x(t)$. The so called frequency response is the magnitude of the transfer function.

In practice, in order to minimize the error over the acquisition of spectra $X(f)$ and $Y(f)$ it is convenient to modify Equation (1.6.15). There are a number of possibilities, one of which is to multiply the numerator and denominator by the complex conjugate of the input spectrum. Thus:

$$H_1(f) = \frac{Y(f) \cdot X^*(f)}{X(f) \cdot X^*(f)} = \frac{G_{xy}(f)}{G_{xx}(f)}. \tag{1.6.16}$$

A second version is found by multiplying with $Y^*(\omega)$ instead of $X^*(\omega)$. Thus:

$$H_2(f) = \frac{Y(f) \cdot Y^*(f)}{X(f) \cdot Y^*(f)} = \frac{G_{yy}(f)}{G_{xy}(f)}. \tag{1.6.17}$$

of the above two forms of frequency response function are amenable to averaging[7].

The $H_1(f)$ frequency response function is used in situations where the output to the system is expected to be noisy when compared to the input.

The $H_2(f)$ frequency response function is used in situations where the input to the system is expected to be noisy when compared to the output.

Chapter 2

General Calibration Procedure and Working principle of a Pressure-Velocity Probe

The device used in this work is composed by two different microphones based on two different principles of transduction: a pressure sensor (PT); and a sensor which directly measures the velocity of the air particle, the dual wires anemometric sensor (VT) (see fig. 2.2.1). A transducer is a device which converts an input signal of a defined form of energy into an output signal of another form of energy. In particular, an electroacoustic transducer transforms voltage variations in an electrical circuit into pressure/velocity variations of an acoustic wave or conversely.

While a pressure sensor can be easily calibrated through a well-established and standard technique involving the usage of a reference microphone of the same kind; for velocity sensors, at present, there are no reference microphones available for the comparison calibration. Hence, a different type of calibration procedure has to be implemented.

For this purpose during the last years different calibration methods have been proposed. Among them is the plane progressive wave method adopted in this dissertation work. It is one of the most robust, even if it requires a large infrastructure for its practical execution.

2.1 Calibration Procedures in Different Reference Fields

As said in the above there is no reference microphone which calibrates the velocity sensor, therefore indirect methods must to be used to calibrate it. Each method has a common base: a field whose impedance is a-priori known, as for instance the impedance in eq.1.3.12. With this assumption and the further knowledge of the true value of pressure, it is possible to calculate the air particle velocity.

This field of a-priori known impedance/admittance will be called in the following the "reference field". Based on this principle, a number of methods have been described in the literature and among them:

- the standing wave tube method, which is efficient only at low frequencies, in a 20 Hz-3.5 kHz bandwidth;
- spherical wave far field method in an anechoic room;
- a piston in a sphere method, in which the probe is put both inside (low frequencies) and outside (high frequencies) a spherical source, and it is calibrated in a free field through two steps for two different range of frequencies [8].

The first two methods, briefly described in the following chapters, have some positives aspects but also some drawbacks. The first method uses an easily transportable device, but it allows analysis only at low frequencies (see sec 2.1.1). While the second method works for all the frequency ranges, it needs an anechoic room for the measurements which means the impossibility to have a transportable calibration device (see sec 2.1.2).

In this case a full range calibration is accomplished and it is not performed inside an anechoic room. The drawback is related to the necessity of making two measurements: one for the high frequencies and one for the low frequencies, and then combine the two obtained spectra in the same graph (see ref. [8]). Moreover there is another problem which all three methods have in common: the dependence on the position; the value measured with each method depend on the specific position of the microphone in the space. Due to this fact and to the necessity to calibrate the probe more easily another method has been developed:

- the progressive plane wave method

which is more simple and practical. This method also has positive and negatives aspects; while it is not possible to calibrate the probe during on site session, the measurements are independent on the position of the microphone. Thid method will be extensively described in section 2.1.3.

2.1.1 The Standing Wave Tube (SWT) Method

A standing wave tube is a closed tube with rigid side walls. Inside it a plane sound wave is generated from a piston and it propagates through the tube until its end where an high percentage

of the sound is reflected back. To have a one dimensional wave, the frequencies of sounds produced have to be below the cut-o frequency:

$$f_s = \frac{c}{1.71d} \tag{2.1.1}$$

where d is the diameter of the tube and c the speed of sound.

The lower frequency limit of the tube is caused by the length of the tube, by the sound probe ttings (the probes should be mounted airtight) and in some extent to the tube diameter. With a $l = 32\,cm$ length and a $d = 5\,cm$ diameter tube, a lower frequency limit of $20Hz$ can be achieved when the probe mountings are airtight.

The specific acoustic impedance inside the SWT can be calculated by solving the wave equation with the appropriate boundary conditions (eq 1.3.12). The air inside is excited by a loudspeaker with amplitude U at the left-hand end, and, at its right hand end, the tube is terminated by a rigid boundary where the reference pressure microphone is inserted, see Figure 2.1.1.

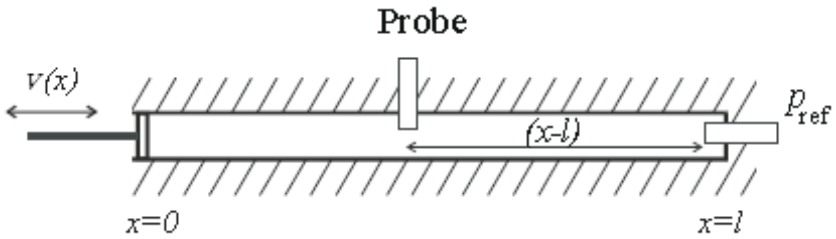

Figure 2.1.1: Standing Wave Tube: A tube that is rigidly terminated at $x = l$ and in which the fluid is driven by a loudspeaker at $x = 0$.

If a pv-probe is put at a certain position x in the tube the relation between the pressure microphone of the pv-probe and the reference (pressure) microphone at the end of the tube is given by:

$$\frac{p_{probe}(x)}{p_{ref}} = cos(k(l-x))$$

The relation turns out to be a simple cosine function.

Analogously, almost the same applies for the particle velocity

$$\frac{v_{probe}}{p_{ref}} = \frac{i}{\rho c}\, sin(k(l-x)) \tag{2.1.2}$$

The relation of the particle velocity and the reference sound pressure at the end of the tube turns out to be a simple sine function. The phase shift between them equals plus or minus 90 degrees.[8].

The formula 2.1.2 is then used to calculate the velocity due to the fact that both the impedance and the pressure are known.

2.1.2 Spherical Wave Far Field Method in an Anechoic Room

If the source can be assumed as a monopole at a distance of r from the observation point then the admittance field can be written:

$$Y_{pv} = \frac{1}{\rho c}\left(1 + \frac{1}{jkr}\right) \tag{2.1.3}$$

where k is the propagation constant equal to $2\pi/\lambda$, where p and v are measured in the same point

The phase shift associated with the finite distance cannot be neglected below a few hundred Hertz even at a distance of 4 m. No ordinary loudspeaker resembles a monopole in its near field, and therefore a distance of several meters is needed. Thus a very special source or a large anechoic room of high quality is required[9]. Knowing the admittance and the pressure inside the field in which the measurements are done the velocity can be calculated through2.1.3.

2.1.3 Progressive Plane Wave Calibration Method

The most simple model of a known impedance field is the progressive plane wave. This field has been realized inside the Larix laboratory: an underground tunnel 100 m long at the University of Ferrara. Inside the tube there is a wave guide which is an aluminium tube$36\,m$ long with a $1,8 \cdot 10^{-2}\,m$ diameter.

Figure 2.1.2: Plane wave guide used for the calibration.

The geometric characteristics of the wave guide guarantee the internal acoustic field to be a progressive plane wave until 10 kHz where the cutoff frequency is calculated through $f_{cutoff} = 0.586\frac{c}{2d}$. Moreover the Larix corridor provides a good homogeneity of environmental conditions, such as humidity and temperature.

The method used for the calibration differs from the other techniques because it is independent

from the position and allows good results in just one set of measurement in wide band, $50-10000$ Hz.

To calibrate the pressure-velocity sensors of the probe two steps are needed

- 1000 Hz calibration of the PT transducer of the probe with a reference pressure microphone;
- calibration of the magnitude and phase of the transfer function of the VT transducer through the correction function $\Gamma(\omega)$.

Calculation ofΓ

The correction function Γ is linked to the VT sensitivity S_{VT} through:

$$S_{VT}(\omega) = \frac{S_{PT}(\omega)}{|\Gamma(\omega)|} \left[Vm^{-1}s\right] \tag{2.1.4}$$

where $S_{PT}(\omega)$ is the PT sensitivity magnitude.

Let's now see how the correction complex function, Γ, can be determined. Let $p^0(t)$ and $v^0(t)$ be the a-priori known pressure and velocity signals in the reference field, and $p_m^0(t)$ and $v_m^0(t)$ their measured values, then these quantities are connected by the expressions

$$p_m^0(t) = (h_{PT} \otimes p^0)(t), \qquad v_m^0(t) = (h_{VT} \otimes v^0)(t) \tag{2.1.5}$$

where $\otimes$ indicates the convolution operator and h_{PT}, h_{VT} are the impulse responses measured by PT and VT. These expressions can be rewritten in the frequency domain as the complex products of the respective Fourier pairs (see eq 2.1.5 and tab 1.6.1):

$$P_m^0(\omega) = H_{PT}(\omega)P^0(\omega), \qquad V_m^0(\omega) = H_{VT}(\omega)V^0(\omega) \tag{2.1.6}$$

from which the pressure and velocity transfer functions can be derived:

$$H_{PT}(\omega) = \left(\frac{P_m^0}{P^0}\right)(\omega), \qquad H_{VT}(\omega) = \left(\frac{V_m^0}{V^0}\right)(\omega) \tag{2.1.7}$$

Due to the reference field conditions we can say that 2.1.7 only depend on the intrinsic characteristics of the sensors and then it can be safely adopted for defining the correction function $\Gamma(\omega)$ as the calibration operator that transform any uncalibrated admittance, $Y_m(\omega)$, measured in any general field conditions in a calibrated measure, $Y(\omega)$.

In fact by putting $\Gamma(\omega) = \frac{H_{VT}(\omega)}{H_{PT}(\omega)}$ one obtains

$$Y(\omega) = \Gamma(\omega)Y_m(\omega) = \frac{H_{VT}(\omega)}{H_{PT}(\omega)}Y_m(\omega) = \frac{V_m^0}{V^0}\frac{P^0}{P_m^0}Y_m(\omega) = \frac{Y^0}{Y_m^0}Y_m(\omega). \tag{2.1.8}$$

where the definition of acoustic admittance is taken into account in the last equation. Thus the explicit form of Γ in term of the a-priori admittance and the measured admittance, is:

$$\Gamma(\omega) = \frac{Y^0}{Y_m^0}. \tag{2.1.9}$$

It is clear that once $\Gamma(\omega)$ is known, the sensitivity of the acoustic velocimeter VT can be corrected according to equation 2.1.4. This process will be implemented and detailed in the next chapter.

Let's finally see how $\Gamma(\omega)$ can be rewritten in the case of a plane progressive wave field.

In this very special case the a-priori admittance of the reference field is just the reciprocal of the characteristic impedance of the air $Y^0 = 1/\rho c$ and thus Γ can be written simply as

$$\Gamma(\omega) = \frac{Z_m^0}{\rho_0 c} \tag{2.1.10}$$

where Z_m^0 is the wave impedance measured in the reference field with the uncalibrated probe.

2.2 Working Principle of the Pressure-Velocity (P-V) Probe

A pressure-velocity probe is made by assembling a pressure (PT) and a velocity sensor (VT), as shown in fig. 2.2.1.

Both the sensors in the probe are acoustic-electrical transducers converting the instantaneous variations of the respective sound quantities to a couple of analogous voltage signals. The PT is an electret microphone: a type of low-cost electrostatic capacitor-based microphone, which eliminates the need for a polarizing power supply by using a permanently charged material.

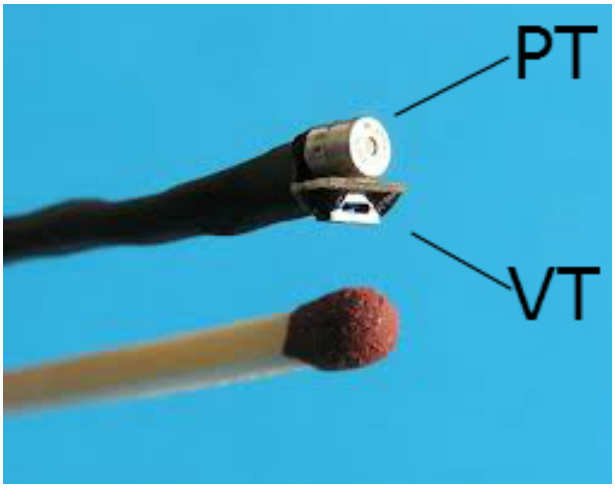

Figure 2.2.1: The Microflown® matchsize probe.

Here below a brief description of the working principle of pressure and velocity transducers is

reported.

2.2.1 Description of the Pressure Transducer (PT)

This kind of sensor is usually called microphone, though we used the same word for the velocity sensor. The transduction element of this microphone is given by a condenser with plane and parallel faces, kept at a constant charge (let's say Q_0) by an external voltage (typically of the order of 200 V). One of the two faces, called diaphragm, consists of a thin metal layer (some μm thick) exposed outside in order to receive the sound pressure oscillations of the nearby field. The entire structure is usually enclosed in a cylindrical capsule as shown in figure 2.2.2.

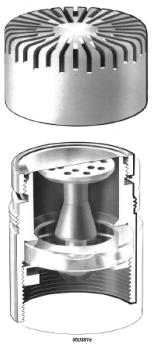

Figure 2.2.2: Classic design of a condenser microphone.

The mechanical vibrations occurring, due to the sound pressure variations, change the rest distance D_0 between the two faces, so that the condenser's capacity changes; therefore, a series of voltage oscillations arise at the two condenser ends, the amplitude of these being linearly dependent on the distance variations d. In fact

$$VC - Q_0 \Rightarrow (V_0 + v)\,\frac{\epsilon_0 S}{D_0 + d} - V_0 \frac{\epsilon_0 S}{D_0} \Rightarrow v - V_0 \frac{d}{D_0}$$

where C is the condenser capacity and v is the voltage fluctuation with respect to the equilibrium value V_0. It is interesting to note that being D_0 quite small, about $20\,\mu m$, the internal field may reach a very high value, that is about $10\,kV/mm$, which is more or less three times the dielectric strength of air: nevertheless, the small distance itself prevents the ion cascade so that no discharge takes place.

An important parameter characterizing the microphone performance is the sensitivity, that is the voltage amplitude corresponding to a given acoustic pressure: it is measured in V/Pa (or in dB relative to $1\,V/Pa$) and usually varies between $1\,V/Pa$ and $100\,\mu V/Pa$. The sensitivity is inversely proportional to the mechanical tension of the diaphragm and directly proportional to its diameter: for instance, the standard microphones of diameter $1,27\,cm(1/2'')$ and $0,64\,cm(1/4'')$

commonly used for intensity measurements, have sensitivities of the order of 12 and 6 mV/Pa respectively [4].

We used as reference microphone, a 1/4 in. B&K® type 4939 and its frequency response is in figure 2.2.3. Brüel&Kjær® normally use 250Hz as the reference frequency. The sensitivity at the reference frequency is used to represent the "overall" sensitivity of the microphone.

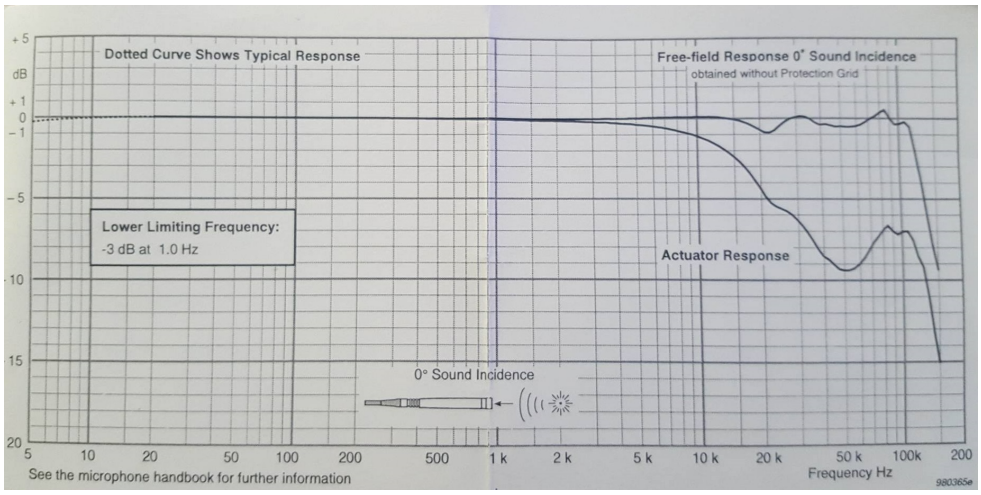

Figure 2.2.3: Brüel&Kjær® frequency response.

An economic version of the condenser microphone is the electrect used in the p-v probe.

2.2.2 Description of the Velocity Transducer (VT)

The transduction principle of the velocity sensor essentially exploits the differential cooling occurring between two wires when exposed to air vibrations due to the propagation of a sound wave (Fig.2.2.6 and 2.2.4). This differential cooling cause a change in the resistance of the wires proportional to the acoustic velocity of the air vibration so allowing a direct measure of the air particle velocity as an electrical voltage signal.

It is important to underline that the thermo-resistant sensors of the Microflown (which are at present the only acoustic velocity sensors available on the market) are implemented with platinum and are heated by an electrical power in order to increase their sensibility.

The two wires of the VT sensor (see fig 2.2.6) have a maximum sensitivity value when exposed orthogonally to the air flow. What is actually measured is the resistance difference between the first and the second wire (Fig. 2.2.5). This oscillation as said before is proportional to the acoustic wind speed.

The variation of the resistors due to sound denoted as ΔR and the non-varying part as R,

the total resistance can be written as:

$$R(t) = R + \Delta R = R\left(1 + \frac{\Delta R}{R}\right) \tag{2.2.1}$$

For two wires with nominal value $R_1 = R_2 = R$ the output voltage signal, U_t, for differential resistance variations equals:

$$U_t = U + \Delta U = \left(1 + \frac{\Delta R_1}{R_1}\right) - \left(1 + \frac{\Delta R_2}{R_2}\right) = 2RI\frac{\Delta R_1}{R_1}. \tag{2.2.2}$$

The common resistance variations are suppressed. The relative differential resistance variation $\Delta R/R$ is defined as:

$$\frac{\Delta R}{R} = \frac{R_1(t) - R_2(t)}{R}. \tag{2.2.3}$$

used in 2.2.2 to calculate the output.

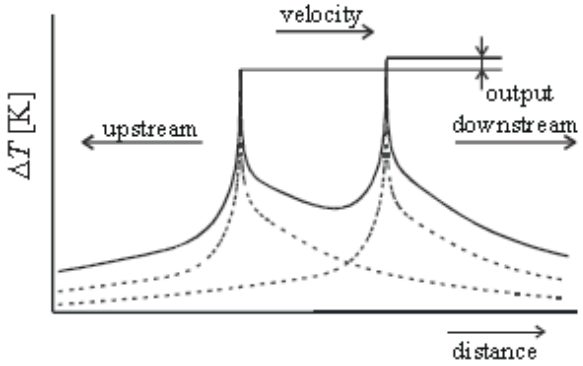

Figure 2.2.4: Dotted lines: temperature distribution due to convection for two heated sensors. Initially both sensors have the same temperature and temperature distribution. Solid line: sum of two single temperature functions: a temperature difference occurs.

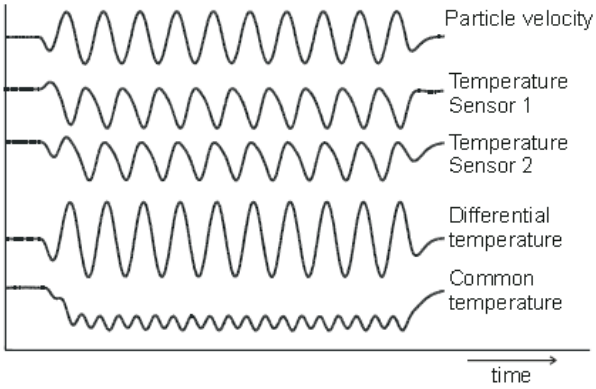

Figure 2.2.5: Measured temperatures of the Microflown® due to an acoustic disturbance. Due to particle velocity both temperature sensors cool down but in a different manner. The temperature difference is proportional to the particle velocity. The sum signal (common signal) represents a sort of hot wire anemometer and measures the common temperature drop. It has an illustrative double frequency that is common for the hot wire anemometry (no discrimination between positive and negative velocity direction).

The Microflown® sensor used is constituted by only one velocity sensor whose axis, i.e. the direction in which the operation is optimal, belongs to the plane in which the threads lie, and is perpendicular to them.

The sensitivity of the velocity sensor, S_{VT} , undergoes a decrease at high frequencies. This is due to the fact that the transport of heat and the thermal capacity of the wires have finite magnitudes.

Taking account of these phenomena and observing a decrease in sensitivity at low frequencies, the correction functions for amplitude and phase of the velocity provided by the manufacturer are:

$$S_{VT}[V/(m/s)] = \frac{S_{VT}@250Hz}{\sqrt{1+\left(\frac{f_{c1v}}{f}\right)^2}\sqrt{1+\left(\frac{f}{f_{c2v}}\right)^2}\sqrt{1+\left(\frac{f}{f_{c3v}}\right)^2}\sqrt{1+\left(\frac{f_{c4v}}{f}\right)^2}} \tag{2.2.4}$$

$$\psi_V[deg] = arctan\left(\frac{C_{1v}}{f}\right) - arctan\left(\frac{f}{C_{2v}}\right) - arctan\left(\frac{f}{C_{3v}}\right) + arctan\left(\frac{C_{4v}}{f}\right) \tag{2.2.5}$$

where $S_{VT}@250Hz$ is the sensitivity of the specific probe to 250Hz, and, f_{civ} and, C_{iv} for $i = 1..4$, are parameters, called *corner frequency*, which uniquely characterize the calibration curve and are determined experimentally. As we can see the S_{VT} is measured in $V/(m/s)$ and to change the sensitivity to mV/Pa^* , the $V/(m/s)$ value needs to be divided according to eq. 1.5.3 for $(\rho \cdot c * 1000 = (343 \cdot 1.2)/1000)$. The reason the sensitivity of the velocity sensor is expressed in mV/Pa^*, is due to the fact that the calibration methods are based on the normalized specific

acoustic impedance: that is the impedance divided by ρc.

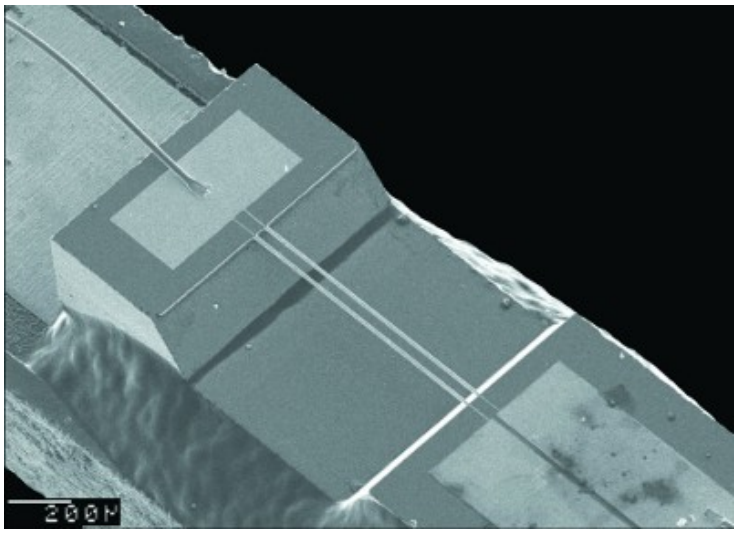

Figure 2.2.6: Particular of the Microflown® velocity sensor: the two thermo-resistant wires.

Chapter 3

Calibration Set-up, Software Tools for Data Acquisition and Analysis

The calibration environment and the main softwares used for the calibration are reported in this chapter. Matlab® and ARTA (Acoustic Real Time Analyzer) are the two software used in this work. The probe is calibrated through the method of the progressive plane wave reference field (see section 2.1.3), with known characteristics. The calibration process has followed different phases:

- calibration of the pressure reference microphone with ARTA;
- calibration of the pressure microphone of the p-v probe with ARTA;
- calibration of the velocity sensor through MATLAB.

3.1 Calibration Environment and Hardware Description

The electro-acoustic measurement chain is illustrated below in figure 3.1.1

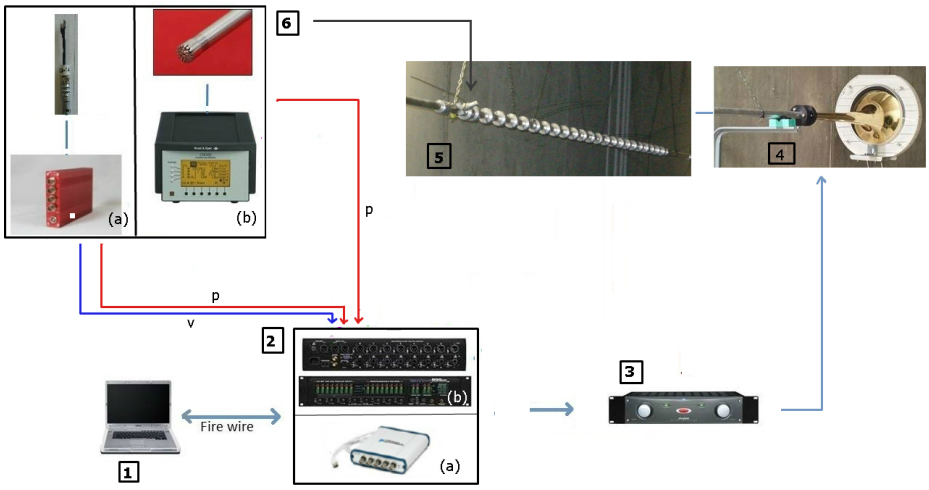

Figure 3.1.1: Experimental Set up used for the calibration of the probes.

It consists of:

1. A portable computer;
2. Audio devices:
   (a) MOTU 896HD audio interface used during the acquisition with ARTA;
   (b) National Instruments®I/O USB data acquisition device (DAQ) (NI USB-4431) has been used with Matlab;
3. Alesis RA150 Amplifier;
4. Tannoy bi-conical loudspeaker (sound source);
5. measurement point, L_0 (aluminium tube).
6. microphones used:
   (a) 1/4 in. Bruel&Kjear® type 4939 (sec. 2.2.1) (reference pressure microphone);
   (b) Microflown® match size p-v probe (sec. 2.2) (probe under test);

The change of A/D-D/A sound card does not affect the procedure of calibration, as its function was just to set the sensitivity of the microphone in ARTA (parameter used just as reference) and to define the absolute dB level of the input signal.

MOTU 896HD

The MOTU 896HD FireWire digital interface provides 18 inputs and 22 outputs, including main out and headphone out. The ports operate at 400 Mbit/s, and they can be connected to any available FireWire port on the computer, fig. 3.1.2a.

NI USB-4431 - 24-Bit Analog I/O

It provides 4 analog input channels and it has a 24-bit resolution for good signal to noise ratio on analog output (AO) and input (AI) channels, fig.

(a) MOTU 896HD.

(b) NI USB-4431.

Figure 3.1.2: Audio devices.

Pressure-velocity Microflown® Probe and pressure Brüel&Kjær® microphone

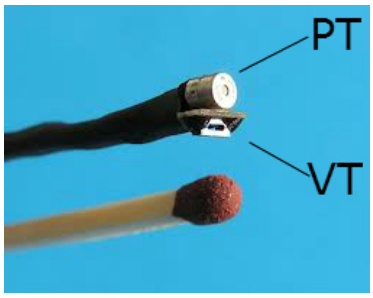

(a) The Microflown® match size probe, where the pressure (PT) and velocity (VT) transducer are highlighted.

(b) 1/4 in. Bruel&Kjear® type 4939, the reference pressure Microphone.

Figure 3.1.3: Transducers used.

Brüel&Kjær® sound Calibrator

The calibration required the use of a B&K® sound calibrator (type 4231). Sound Calibrator Type 4231 is a pocket-sized, battery operated sound source for quick and direct calibration of sound level meters and other sound measuring systems. It fits Brüel & Kjær 1″ microphones and

using the removable adaptor, 1/2″ microphones. With optional adaptors, it can be used for 1/4″ and 1/8″ microphones as well. The calibration frequency is 1000 Hz (the reference frequency for the standardized international weighting networks). The calibration pressure of 94 ±0.2 dB re 20 µPa is equal to 1 Pa or 1 N/m2. The +20 dB level step gives 114 dB SPL, which is convenient for calibration in noisy environments, or for checking linearity.

Figure 3.1.4: Sound calibrator.

Tannoy bi-conical loudspeaker and the Measurement point, L_0 (Aluminium Tube)

The measurement point consists of a long aluminium tube, coupled at one end with a Tannoy bi-conical loudspeaker (left image in Fig. 3.1.5), it allows to reproduce a wide range of frequencies $50 - 15000\ Hz$. A modified trombone bell, used as an impedance adapter (right image in Fig. 3.1.5), grants an optimal SPL level of the field in the measurement point.

Figure 3.1.5: Sound source and impedance adapter.

The aluminium tube is 36 m long and its diameter measures $1,8 \cdot 10^{-2}\, m$, the tube was assembled by combining 6 m long modules (Fig. 3.1.6b), connected by appropriate fittings and hung with chains so as to adjust and maintain the axial alignment, obtained by means of a laser beam.

It is possible to calculate the frequency cut-off knowing the diameter of the tube, above which appear modes of transverse oscillations, according to the formula: $f_{cutoff} = 0.586\frac{c}{d} \approx 10\, KHz$.

One of the modules has been perforated with holes at 20 cm distance one from the other to allow the insertion of the probe inside the tube; each hole is airtight when not used; in our case the probe was inserted in the last hole of he pipe at $10.80\, m$ from the source to assure a good signal to noise ratio. The tunnel ensures homogeneous moisture and temperature conditions of the entire tube by minimizing the influence of any external variation, in figure **??** the tube and the set up used.

(a) Part of the tube for the insertion of the probe.

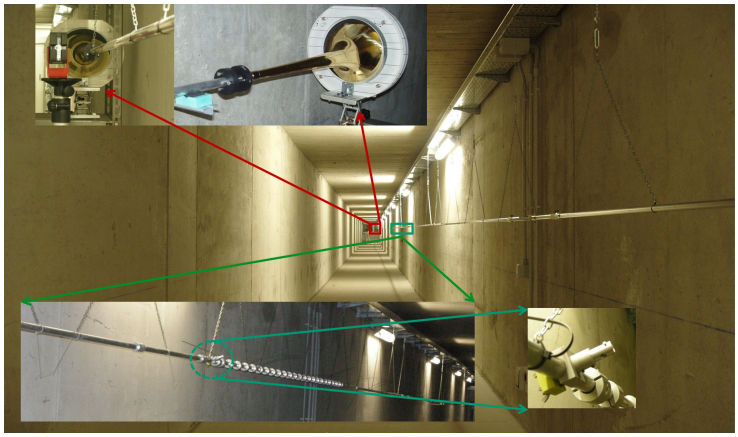

(b) Larix.

Figure 3.1.6: Set up of the Larix laboratory.

3.2 Description of the software for Data Acquisition and Post-Processing

Two main softwares have been used for the calibration process: ARTA (Acoustical Real Time Analyzer) and Matlab. While ARTA is a proprietary software, Matlab® is a high-level language which gives the chance to define a routine that can be modified depending on the situation and on what is needed for the analysis, which perfectly fits the purposes of this work.

3.2.1 Acoustic Real Time Analyzer - ARTA

ARTA (Acoustic Real Time Analyzer) is a software for impulse response measurement, real-time spectrum analysis and real-time measurement of the frequency response. We used it as a real-time analyzer [7]. In the figure 3.2.1 below is reported the impulse response acquired by the Brüel&Kjær® microphone through ARTA in L_0.

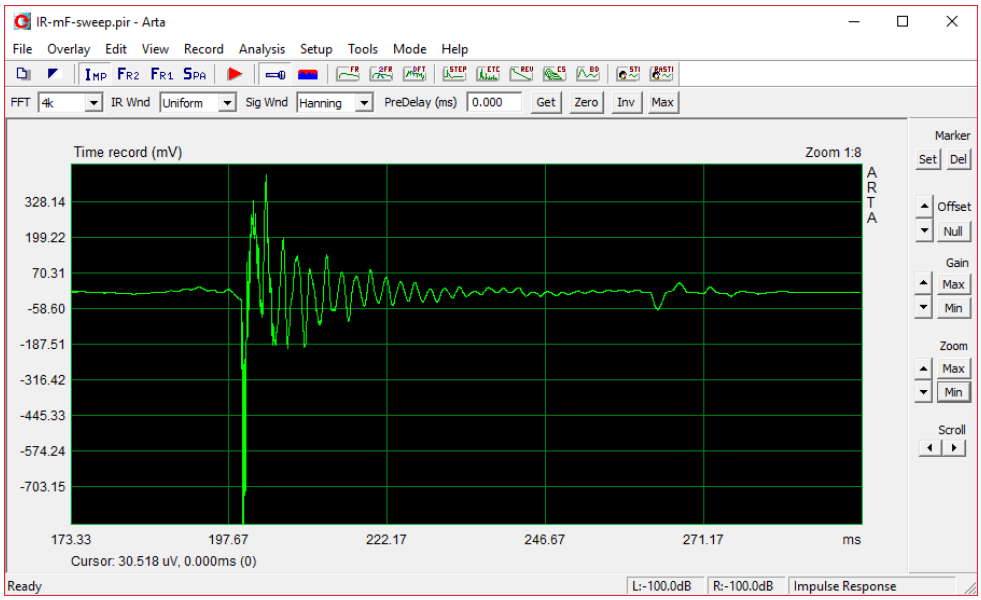

Figure 3.2.1: ARTA interface, example of acquisition of an impulse signal with the Brüel&Kjær® microphone in L_0.

3.2.2 Matlab®

Matlab® is a high-level language and interactive environment which is used in many fields. This project has involved different already built routines of Matlab®:

- Sweep4Calib application;
- cftool application;
- tfestimate function.

3.2.2.1 Sweep4Calib

The Sweep4Calib is a routine that was originally written to calculate the impulse response of a 4 channel p-v 3D probe and then modified to calculate only the impulse responses of the two signals of pressure and velocity of a 1D axial probe (fig. 3.1.3a). In this work the routine was just used as sound wave generator and recorder. The routine was specifically though for the measurements made inside the Larix laboratory.

As can be seen in figure 3.2.3, the Sweep4Calib routine requires different input parameters such as the humidity and room temperature, which were both acquired by using a special pen-drive for 17 hours continuously. The results are shown in the following chart (Fig.3.2.2) .

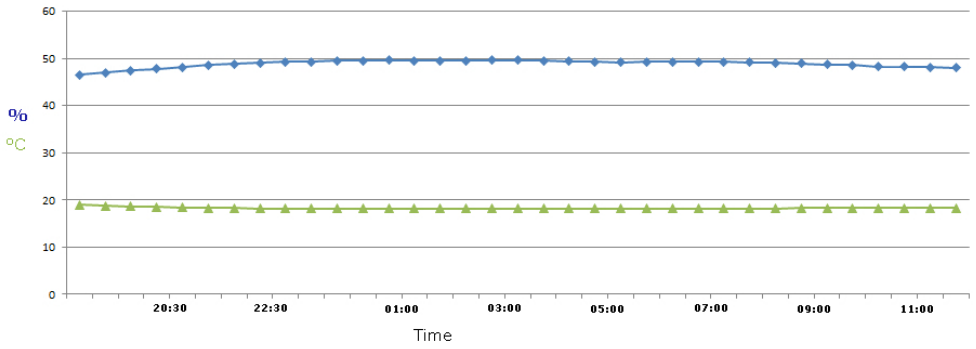

Figure 3.2.2: Temperature (green line, °C) and Relative Humidity (blue line, %) in Larix Laboratory.

As clearly plotted on the graph, these two parameters have always approximately the same value, $(18.5 \pm 0.1)^\circ$ for the temperature and $(48 \pm 1)\,\%$ for the relative humidity, they will be used as environmental parameters while defining the signal (see figure 3.2.3). Due to this peculiarity of the tunnel the sound velocity is practically constant (see sec.1.2) in the range of 340.27 and 343.21 m/s, in our case 342.8 m/s, and also the product ρc, reported in table 3.2.1 below, these parameters will be used during the analysis.

Temperature T (°C)	Speed of sound c (m/s)	Density of air ρ (kg/m^3)	Characteristic specific acoustic impedance z_0 (Pa·s/m)
35	351.88	1.1455	403.2
30	349.02	1.1644	406.5
25	346.13	1.1839	409.4
20	343.21	1.2041	413.3
15	340.27	1.2250	416.9
10	337.31	1.2466	420.5
5	334.32	1.2690	424.3
0	331.30	1.2922	428.0
−5	328.25	1.3163	432.1
−10	325.18	1.3413	436.1
−15	322.07	1.3673	440.3
−20	318.94	1.3943	444.6
−25	315.77	1.4224	449.1

Table 3.2.1: Effect of temperature on the characteristic impedance of air.

The software allows the user to define a signal through the command window in figure 3.2.3, it also allows to set others parameters useful for the process and the post process analysis, for example the identification of the probe used through the "Transducers settings" buttons.

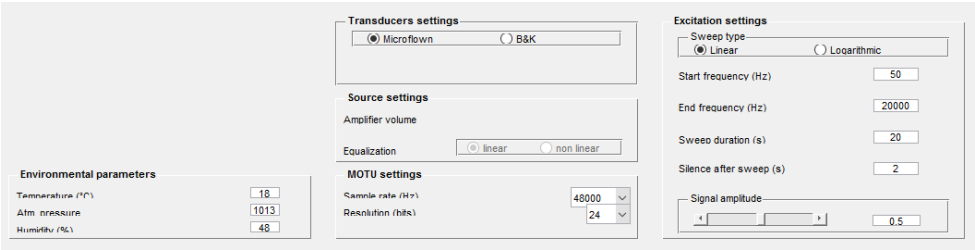

Figure 3.2.3: User interface of the Sweep4Calib routine implemented with Matlab®.

The sampling frequency is set to 48000 Hz, the only thing that changes is the frequency of the sound wave, which is set at first to 1000 to have a pure tone signal, and then from 50 to 20000 to obtain a full range frequency signal, to calibrate the VT transducer of the probe.

Due to the fact that saving a file to a "wav" type imply its normalization and the loss of some information, the Sweep4Calib routine save them as additional information in the header of the ".wav" file. One of the information stored in the header is the maximum amplitude value of the signal, labeled as "maxr", which will be used during the analysis in the Matlab® routines to obtain the true amplitude of the signal, code reported in Appendix A.

3.2.2.2 Cftool

The Curve Fitting app provides a flexible interface where the user can interactively fit curves and surfaces to data and view plots. Thanks to this tool, it is possible to:

- create, plot, and compare multiple fits;
- use linear or nonlinear regression, interpolation, smoothing, and custom equations;
- view goodness-of-fit statistics, display confidence intervals and residuals, remove outliers and assess fits with validation data;
- automatically generate code to fit and plot curves and surfaces, or export fits to the workspace for further analysis.

The application gives the possibility to use an algorithm and a type of robust estimate which allows to find the best fitting parameters for a custom curve defined by the user. The algorithm used is a trust-region least squares algorithm. The basic idea behind it is to approximate a function, $f(x)$, with a simpler function q, which reasonably reflects the behavior of function f in a neighborhood N around the point x. This neighborhood is the trust region. Furthermore the trust region is used with the constrain that the corner frequencies need to be positives which optimize the choice of parameters, a deeper explanation of it could be found in [10].

The robust fitting with bisquare weights estimate uses an iteratively reweighted least-squares algorithm[1], a visual example of the method can be seen in the plot shown below which compares a regular linear fit with a robust fit using bisquare weights. Notice that the robust fit follows the bulk of the data and is not strongly influenced by the outliers (more information in [11]).

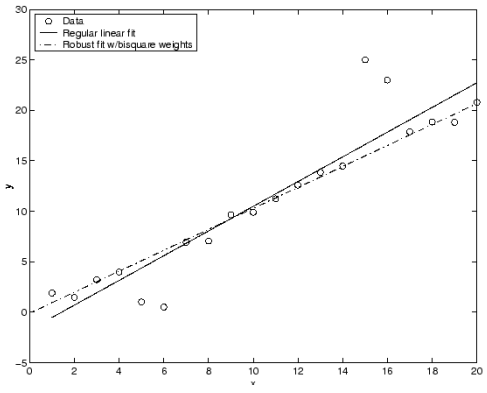

Figure 3.2.4: Comparison between a regular linear fit and a robust fit (dotted line) using bisquare weights.

[1]This method minimizes a weighted sum of squares, where the weight given to each data point depends on how far the point is from the fitted line. Points near the line get full weight. Points farther from the line get reduced weight. Points that are farther from the line than would be expected by random chance get zero weight [11].

3.2.2.3 Tfestimate

Compute and plot the transfer function estimate between two sequences, x and y.

$$Gamma\_fft = tfestimate(x,\ y,\ window,\ noverlap,\ nfft,\ Fs)$$

$nfft$ FFT length which determines the frequencies at which the PSD is estimated;

window Windowing function and number of samples to use to section x and y;

Fs Sampling frequency;

noverlap Number of overlap samples.

The relationship between the input x and output y is modeled by the linear, time-invariant transfer function $H_1(\omega)$. The transfer function, as defined in eq 1.6.16, reported below, is the quotient of $G_{xy}(\omega)$, the cross power spectral density of x and y, and $G_{xx}(\omega)$, the power spectral density of x:

$$H_1(\omega) = \frac{Y(\omega) \cdot X^*(\omega)}{X(\omega) \cdot X^*(\omega)} = \frac{G_{xy}(\omega)}{G_{xx}(\omega)}$$

3.3 Execution of the Calibration Procedure for the Pressure-Velocity Probe Under Test

This section contains the detailed description of the procedure which has followed the steps already defined in the main introduction of the chapter.

3.3.1 Calibration of the Pressure Reference Microphone at 1000 Hz

In the first step of the procedure, a sound calibrator is used to calibrate the Brüel&Kjær® type 4939 to use it as the reference microphone for the whole calibration process; when using calibrators that produce a single frequency, the calibration is only valid at this nominal frequency. However, Brüel&Kjær® type 4939 has a flat frequency response, which means that it gives the same electrical output at all frequencies. Therefore, calibration at a single frequency is sufficient in most situations and the calibration should be considered valid for all the other frequencies.

The pressure reference microphone has been inserted inside the sound calibrator and due to the fact the calibrator has a known sound level of 94 dB_{SPL} it is possible to set the input gain of the microphone in ARTA to obtain a RMS level that is exactly equal to the emitted value.

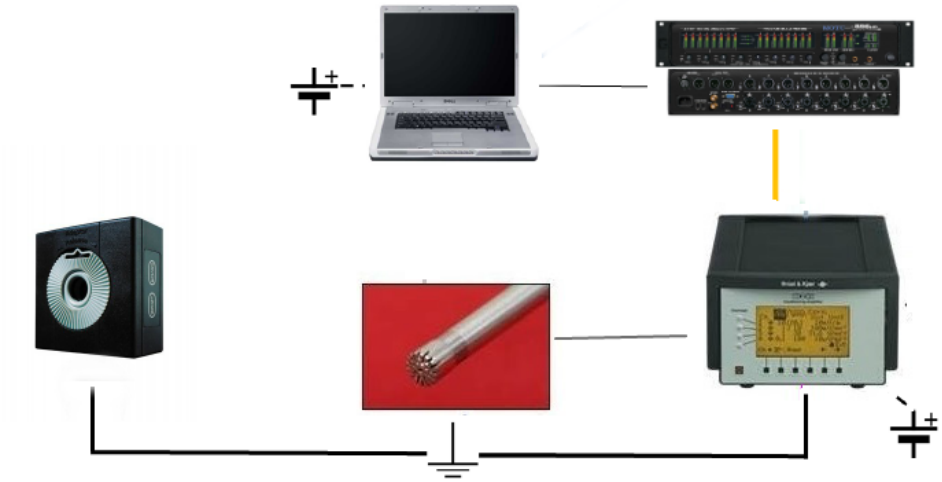

Figure 3.3.1: Set up calibration with the sound calibrator.

3.3.2 Calibration of the Pressure Microphone of the Probe at 1000 Hz

In each situation the Sweep4Calib routine has been used as sound generator, the set up calibration is shown in figure 3.1.1. During this step a 1000 Hz signal has been generated and emitted through the loudspeaker while firstly the reference pressure microphone B&K®, already calibrated, and sub sequentially the Microflown® have been inserted into the last hole of the pipe at 10.80 m from the source to acquire the signal and measure the response of the system. For the B&K

microphone only the "vents" of the transducer are inside the tube to avoid excessive turbulence events. With the reference microphone is possible to measure with ARTA the true dB level of the signal which has been found approximately of $(88 \pm 1)\, dB_{SPL}$.

The value obtained is kept as reference while measuring the pure tone signal with the Microflown® pressure probe comparing it with the value acquired by the probe under test and defining the correct value of sensitivity, this value will be then compared with the result obtained through the Matlab® routine and eq 2.2.4.

3.3.3 Calibration of the Velocity Sensor at 1000 Hz

As already explained in 2.1.3 the value of velocity is obtained through the calculation of the gamma function and the calibrated pressure signal.

Due to the properties of the reference field, whose impedance is equal to ρc, the values of velocity and pressure measured have to be equals when the velocity is measured in Pa^* (see section 1.5.2) and then both the sensor needs to have the same dB level at that frequency.

First of all, it is necessary to choose the same measurements units both for velocity and pressure data. From the dB_{SPL} level measured it is possible to obtain the relative pressure value in Pascal (section 3.3.2), using the inverse formula of 1.5.1

$$P_{rif}(Pa) = 20 \cdot 10^{-6} \cdot 10^{(dB\ Level\ Measured\ ARTA/20)}. \tag{3.3.1}$$

Sensitivity is calculated through the formula

$$S_{PT} = P_{measured}/P_{rif} \tag{3.3.2}$$

thus obtaining for the sensitivity of the Microflown® pressure microphone the following value $S_{PT}(1000) = 37.9\, mV/Pa$. The value of $S_{PT}(1000)$ obtained is similar to the one given by the manufacturer of the probe which is equal to $37.4\, mV/Pa$.

In this work to obtain the corrected sensibility for the pressure probe at each frequency we applied the correction curve given by the manufacturer for the amplitude, eq 3.3.3, of the probe

$$S_{PT}(\omega)\ [mV/Pa] = S_{PT}@1kHz \frac{\sqrt{1 + \left(\frac{f}{f_{c3p}}\right)}}{\sqrt{1 + \left(\frac{f_{c1p}}{f}\right)}\sqrt{1 + \left(\frac{f_{c2p}}{f}\right)}} \tag{3.3.3}$$

$$\psi_{PT}[rad] = arctan\left(\frac{C_{1p}}{f}\right) + arctan\left(\frac{C_{2p}}{f}\right) + arctan\left(\frac{f}{C_{3p}}\right) \tag{3.3.4}$$

where f_{cip} and C_{ip}, with $i = 1, 2, 3$ are the corner frequencies given by the manufacturer, reported in the table 3.3.1 below:

Sensitivity		
S_{PT}@1000Hz	37.4	$[mV/Pa]$
Sensitivity Cornerfrequencies		
f_{c1p}	32	Hz
f_{c2p}	44	Hz
f_{c3p}	16946	Hz
Phase cornerfrequencies		
C_{1p}	37	Hz
C_{2p}	32	Hz
C_{3p}	50865	Hz

Table 3.3.1: Corner frequency for the pressure correction curve given by the constructor in [5].

3.3.4 Calculation of the Frequency Dependent Sensitivity of the Velocity Sensor and Obtained Results

To obtain the correction function a sweep signal between 50-20000 Hz is produced and its response is acquired both with the Brüel&Kjær® pressure microphone and the Microflown® probe in L_0. This is done to assure a full range calibration for the VT due to the fact it doesn't have a flat response.

The procedure detailed in this subsection follows the scheme reported in section 2.1.3. The $\Gamma(\omega)$ function, obtained through eq 2.1.10 and reported below, can be used to calculate the sensitivity of the velocity sensor in the plane progressive reference field as follow [12]:

$$\Gamma(\omega) = \frac{Z_m^0}{\rho_0 c} \tag{3.3.5}$$

where Z_m^0 is the impedance measured in the reference field. It is now possible to obtain the sensitivity of the velocity channel:

$$S_{VT}(\omega) = \frac{S_{PT}(\omega)}{\Gamma(\omega)}. \tag{3.3.6}$$

The formula 3.3.6 is the one that connects the sensitivities of pressure and velocity transducers that are expressed in the same measurement units..

3.3.4.1 Data Post-Processing

The correction function $\Gamma(\omega)$ is determined with Eq. 3.3.5, and Z_m^0 has been calculated with the tfestimate function of Matlab® (see section 3.2.2), which is defined as follows

$tfestimate(x,\ y,\ hanning(\#\ of\ samples),\ \%\ of\ overlap,\ \#\ of\ samples,\ Sampling\ frequency)$

where x and y are the are the measured signals taken with the Microflown® probe under test (PUT), they indicate respectively pressure and velocity. As already stated in section 3.2.2, the function computes the following ratio:

$$H_1(\omega) = \frac{Y(\omega) \cdot X^*(\omega)}{X(\omega) \cdot X^*(\omega)} = \frac{G_{xy}(\omega)}{G_{xx}(\omega)}$$

which is essentially the admittance measured with the uncalibrated probe.

The equation of the Gamma is then modified in the following way

$$\Gamma(\omega) = \frac{1}{\rho_0 c \cdot H_1(\omega)}. \tag{3.3.7}$$

In Fig. 3.3.2 the magnitude and phase of the $\Gamma(\omega)$ obtained through the Matlab® code reported in Appendix A

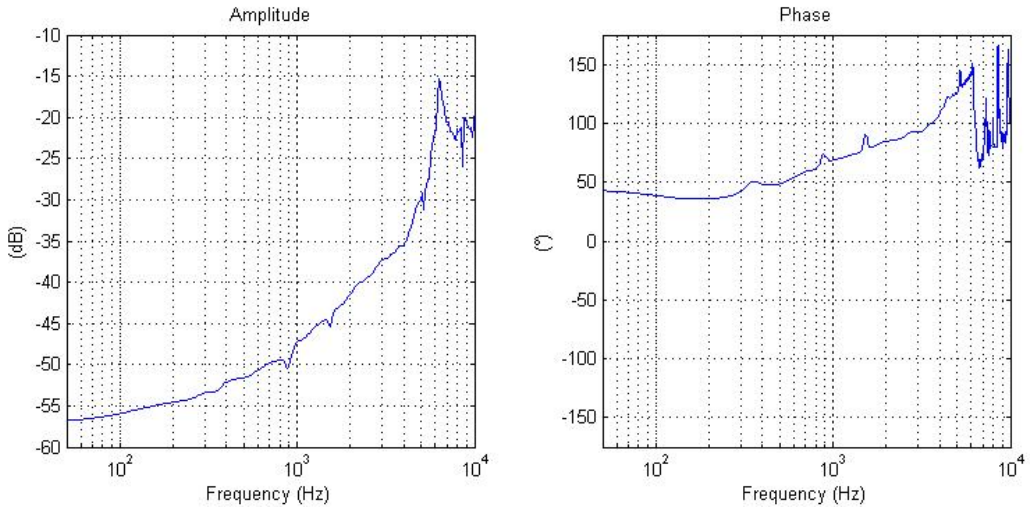

Figure 3.3.2: Magnitude and phase of the $\Gamma(\omega)$ obtained through the Matlab® code implemented.

Comparing the curves in 3.3.2 with those reported in [1] obtained with a similar procedure and with a similar probe (a different prototype), it is possible to verify that they have very similar trends which underline the goodness of the procedure.

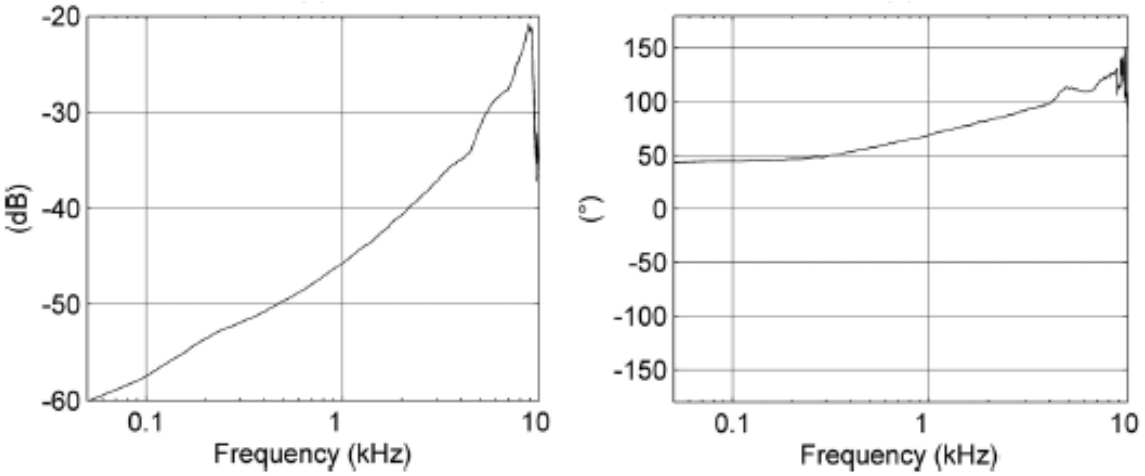

Figure 3.3.3: Gamma function reported in [1]. In the left graph the amplitude and in the right the phase.

Finally, we can also calculate the sensitivity of the velocity probe (VT) $S_{VT}(\omega)\, Vm^{-1}s$ using 3.3.5 which can be rewritten as

$$S_{VT}(\omega) = \left|\Gamma^{-1}(\omega)\right| S_{PT}(\omega)\, Vm^{-1}s \tag{3.3.8}$$

where $S_{PT}(\omega)$ is the frequency dependent nominal sensitivity given by the manufacturer. The results obtained with this formula, in green, are compared with the nominal ones given by the calibration curve of the Microflown® report, in blue, (see eq. 2.2.4 and [5] to know more) in figure 3.3.4a.

3.3.5 Comparison between the Nominal and the Experimental Calibration

Referring to the previous section the formula 3.3.8 has been introduced this formula is going to be used to obtain the experimental data for the sensitivity correction. The experimental data obtained will be used to calculate the analytical curve through their interpolation and finding the right corner frequencies of the curve given by the Microflown® report. Below the description of the steps made to obtain those curves and the graph obtained.

The calibration curves needed to calibrate the VT sensor of the probe, both in amplitude and phase, are here reported:

$$S_{VT}[V/(m/s)] = \frac{S_{VT}@250Hz}{\sqrt{1+\left(\frac{f_{c1v}}{f}\right)^2}\sqrt{1+\left(\frac{f}{f_{c2v}}\right)^2}\sqrt{1+\left(\frac{f}{f_{c3v}}\right)^2}\sqrt{1+\left(\frac{f_{c4v}}{f}\right)^2}} \tag{3.3.9}$$

$$\psi_{VT}[rad] = arctan\left(\frac{C_{1v}}{f}\right) - arctan\left(\frac{f}{C_{2v}}\right) - arctan\left(\frac{f}{C_{3v}}\right) + arctan\left(\frac{C_{4v}}{f}\right) \tag{3.3.10}$$

The sensitivity value at 250 Hz is obtained through the following formula $S_{VT}(250Hz) = |\Gamma(250Hz)|^{-1} S_{PT}(250Hz) V m^{-1} s = 11.87\, V/(m/s)$.

As can be seen in [5] and in the equations 3.3.9 and 3.3.10, the Microflown® defines a calibration curve for the velocity probe, where some parameters, called "corner frequencies", describe the calibration curve.

Through Matlab® and its routine "cftool" (see sec.3.2.2) it is possible to find out the corner frequencies related to the experimental data obtained through the equation 3.3.8 and calculate the right velocity for both amplitude and phase.

The table below shows the the corner frequencies obtained with the Matlab® routine and those of the Microflown® calibration report [5]. The two sets of the corner frequencies have been used to obtain the respective curves in figure 3.3.4a

Sensitivity in low gain		
S_v@250Hz	11.87	$[V/(m/s)]$
Sensitivity cornerfrequencies		
f_{c1v}	26.97	Hz
f_{c2v}	4462	Hz
f_{c3v}	690.8	Hz
f_{c4v}	26.97	Hz
Phase cornerfrequencies		
C_{1v}	16.3	Hz
C_{2v}	684.8	Hz
C_{3v}	13470	Hz
C_{4v}	7.46	Hz

(a) Corner frequencies obtained through the best fitting procedure from experimental data.

Sensitivity in low gain		
S_v@250Hz	12.5	$[V/(m/s)]$
Sensitivity cornerfrequencies		
f_{c1v}	142	Hz
f_{c2v}	573	Hz
f_{c3v}	4281	Hz
f_{c4v}	1	Hz
Phase cornerfrequencies		
C_{1v}	113	Hz
C_{2v}	625	Hz
C_{3v}	8030	Hz
C_{4v}	1	Hz

(b) Corner frequencies given by the Microflown® report[5].

Table 3.3.2: Corner Frequencies.

As can be seen in figure 3.3.4a the nominal and best-fitted amplitude filters have a very similar behavior.

The results for the dB levels and phase obtained are reported in Fig. 3.3.4a and 3.3.4b where the following three plots are represented: (1) blue line: analytical corrections from Eqs. 3.3.9 and 3.3.10 with, $F_{i=1,4}$, $C_{i=1,4}$ and $S_{VT}@250Hz$ set to the nominal values, in the graph defined as nominal curve; (2) green line: experimental corrections from $\Gamma(\omega)/S_{PT}(\omega)$, experimental curve; and (3) red line: best-fitted analytical corrections best-fitted from experimental data using Eqs.3.3.9 and 3.3.10 with $S_{VT}@250Hz \equiv 11.87\, V/m^{-1}s$, analytical curve.

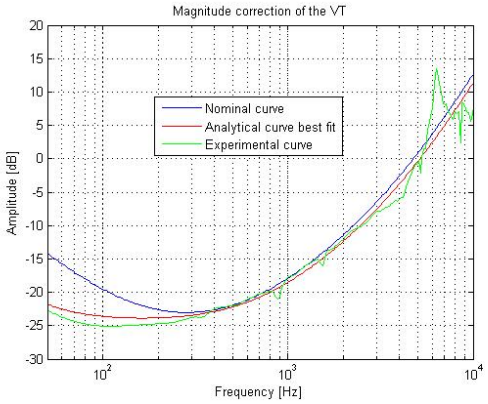

(a) Blue line: nominal curve from the equation 3.3.9; Green line: experimental curve from $\Gamma(\omega)/S_{PT}(\omega)$; Red line: optimized filters by best-fitting experimental data with the analytical model curve.

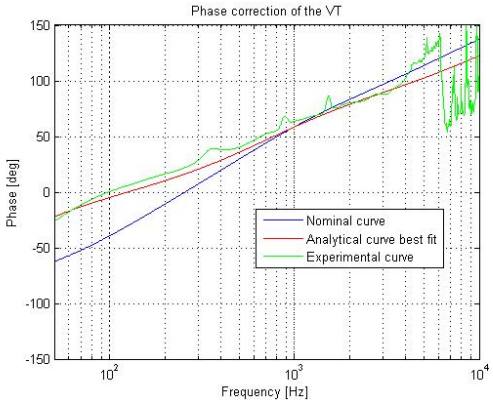

(b) Phase correction filter. Blue line: nominal filters; Green line: experimental filters; Red line: optimized filters by best-fitting experimental data with the analytical model curve.

Figure 3.3.4: Magnitude and Phase correction correction of equations 3.3.9 and 3.3.10, with the parameters given by the Microflown® report. Curves compared with the experimental correction curve given by3.3.8. $S_{PT}(\omega)$ is determined by equations 3.3.3 and 3.3.4 and $\Gamma(\omega)$ through equation 3.3.7.

Again in Fig. 3.3.4a the nominal and best-fitted amplitude filters have a similar behavior but as stated before, there is an increasing difference under 200 Hz. The discrepancy observed is due to the fact that it has been used the correction curve of the Microflown® with the parameters given by their report, while there is although a little difference between the sensitivity of the report and the one calculated. At high frequencies the procedure and the curve fitting are good and the analytical curve fits the nominal one.

The calibration of the phase is computed with the same procedure explained for the amplitude where the phase of the $\Gamma(\omega)$ function is obtained and equation 3.3.4 has been used to obtain the correction for the sensitivity phase of the pressure probes, in figure 3.3.4b the results obtained.

In figure 3.3.5 the results obtained in [1] to allow a direct comparison between the graphics obtained

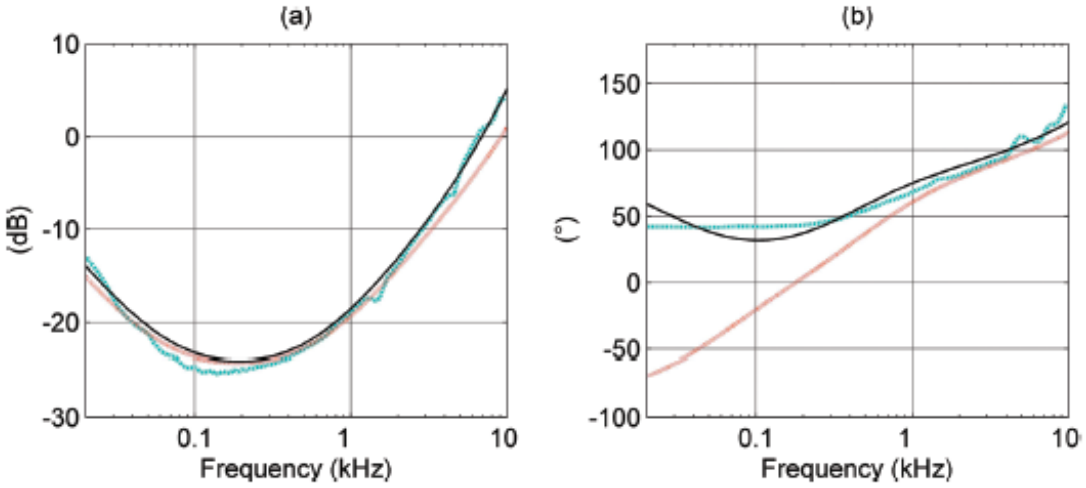

Figure 3.3.5: Magnitude and Phase correction correction of equations 3.3.9 and 3.3.10, with the parameters given by the Microflown® report. The amplitude curve is compared with the experimental correction curve given by 3.3.8. $S(\omega)$ is determined by the comparison of the Microflown® probe with the reference probe and $\Gamma(\omega)$ through equation 3.3.7. Whereas the comparison of the phase correction curve was done simply with the PT phase response.

The results obtained in figure 3.3.4 compared with the one in [1], figure 3.3.5, have similar behavior in amplitude which underline the goodness of the procedure. The phase correction curve obtained in this work has a better fitting compared to the one in [1], due to the fact it has been used the pressure calibration curve of the phase given by the manufacturer instead of the effective phase of the probe, as it had been done for the curve in figure 3.3.5. As can be seen in both phase correction graph, there is a noticeable difference under 1300 Hz between the curves obtained and the one of the Microflown®, confirming the results obtained in [1].

Chapter 4

Conclusions and Future Applications

This chapter presents a quick overview of all the dissertation and some considerations on the work that has been done. Moreover, the last section contains a brief description of a new prototype probe and a generalization of the above presented method for its calibration.

4.1 Summary and Concluding Remarks

This section summarizes the topics covered in the dissertation.

The first chapter deals with the theory that is behind the process of sound propagation, which is what all the acoustic theories are based on. The first section is about the wave equation, the way it is obtained and its solutions in the cases of standing and traveling sinusoidal waves of sound. Afterwards, two physical quantities that are important for the analysis are introduced: the admittance and the impedance. Moreover, this section contains a brief discussion on the measurement units that define the different sound levels, i.e. the decibel scale, for the following different quantities: sound pressure level (SPL), particle velocity level (AVL) and sound intensity level.

A section has been totally devoted to one of the most important topics of the applied acoustic: the Fast Fourier transform. It has been described giving importance also to some functions related to it which are at the base of the sound analysis and used during the elaboration of sounds, i.e. cross-spectrum and transfer function.

The second chapter introduces some calibration procedures. The Standing Wave Tube (SWT) method and the spherical wave far field method in an anechoic chamber are briefly presented to define their positive and negative aspects and are compared with the method used in this dissertation, which is the progressive plane wave. The last section describes the transduction principles of the microphones that have been used, i.e. pressure and velocity. In particular, as the VT is a new type of transducer, a calibration procedure for this sensor must be found.

Finally, the last part is about the analysis and programming procedures that have been

followed to obtain the data and graphs. The set up used for the calibration is described and particular attention is given to the software and the set up used. Moreover, this part includes a quick overview of the hardware needed and a more accurate description of the software that have been used, i.e. ARTA and Matlab, as well as some proprietary routines of the latter. The results obtained show that the data fit well with the nominal ones and that the written routine allows a direct comparison with all the data.

In the first chapter is explained all the theory needed to understand the acoustical process faced. In the second one different procedures of calibration are reported with a particular attention to the one used, and also great importance is given to the transduction principles of the microphone used. Due to the simple acoustic properties of the here-chosen reference field and its physical implementation by means of a one-dimensional acoustic wave guide in a highly controlled environment, the method offers great functional versatility in all phases of the proposed calibration procedure. The calibration facility allows one to get results of experimental precision and robustness comparable with the usual comparison calibration method practically adopted for pressure microphones.

Finally in the last chapter the data have been acquired and analyzed beginning with the calibration of the pressure probe of both the devices. The obtained pressure sensitivity of the Microflown® sensor has been compared to the one defined by the manufacturer to verify the possibility to use the curve given by the report to have a calibrated signal of pressure.

After this first step the gamma curve has been calculated considering the uncalibrated signals of pressure and velocity. Then the sensitivity of the velocity probe is given through the experimental correction given by the formula 3.3.8. The data obtained have been used to obtain the parameters of the curve given by the manufacturer but best fitted on the experimental data, both for amplitude and phase. As already underlined the amplitude correction is good while for the phase there is a visible difference under 1300 Hz. This difference is due to the fact that the correction curve for the phase is obtained through the gamma, which has been calculated by the uncalibrated impedance. Has already reported in [1], and here confirmed, the comparison of the phase correction curves shows a significant deviation of the nominal curve with respect to the experimentally calculated filter just for low frequencies under 1300 Hz.

The procedure explained in this work and the Matlab® routine produced are very helpful for future developments of the calibration procedure of the probe, thanks to the usability of the software and to its possibility to change the code, depending on the conditions of operation. Moreover, the procedure used for the calibration is said to be trustworthy and could be implemented for all the frequency range of the pressure microphone probe.

4.2 Future applications

The laboratory of Ferrara (Italy) in collaboration with the IIEIT (Institute of Electronics, Computer and Telecommunication Engineering) of Pisa (taly) and the town of Sogliano al Rubicone (Italy) have developed a new type of p-v probe which is based on the same working principle of the Microflown® one but it uses a different technology CMOS. The CMOS technology has a lower cost compared to the one of the Microflown® and and it is made with a standard process of construction.

The construction of this prototype is part of a project named SIHT (Sogliano Industrial High Technology).

4.2.1 4.1.1 CMOS Compatible p-v Probes

Complementary metal–oxide–semiconductor (CMOS) is a technology for the construction of integrated circuits. CMOS technology is used in microprocessors, microcontrollers, static RAM and other digital logic circuits, such as microphones.

The velocity sensor has been realized by the CNR-IEIIT-Pisa (Italy) in collaboration with the Department of Information Engineering of the University of Pisa. The device consists of two micro- heaters integrated in a silicon chip and works by transferring heat from one heater to the other through the orthogonal propagation of the acoustic wave. If any acoustic signal is transmitted, the two heaters are maintained at the same temperature: the air movement that propagates orthogonally to the heaters defines a heat transfer between the heaters and a variation of their temperature, which is detected through the measurement of the variation of their resistance.

The two heaters are made of two polysilicon resistors positioned on suspended membranes of silicon oxide. The structure has been realized through silicon micromachining techniques that are used for the creation of integrated micro-electromechanical systems (MEMS). In particular, the chip that contains the sensor is designed with a commercial CMOS process of the STMicroelectronics and has been realized with the post-processing technique. This technique works on the chip as it creates suspended structures such as membranes when leaving the foundry. For this work, it was necessary to create cavities in the silicon chip in order to thermally isolate the heaters from the substrate. Details concerning the manufacturing process can be found in [13].

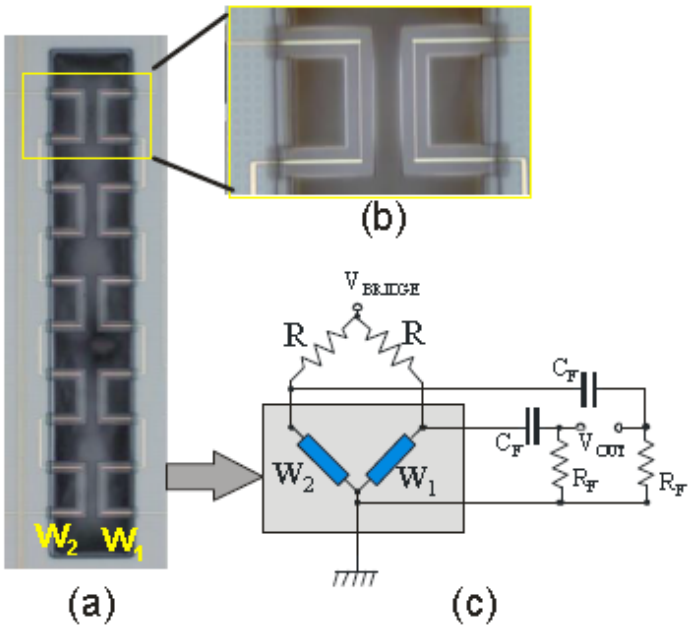

Figure 4.2.1: (a)Photo at the optical microscope of the acoustic particle velocity sensor realized in CMOS technology. (b) Magnification of one of the five sections in which each heater has been divided into. (c) Scheme of the circuit used for the test of prototypes.

Figure 4.2.1(a) shows a photo at the optical microscope of the two heaters (W1 and W2): each heater has been divided into five sections in series to give robustness to the structure, each of which is positioned on a oxide silicon "shelf" suspended above the cavity. The magnification of Figure 4.2.1 (b) shows the detail of one of the five sections of the two heaters: the distance between the two heaters is $10\,\mu$ m . It is possible to integrate in the same chip both the sensor and the electronic circuits for the detection and processing of the signal. This is due to the kind of process used for the realization of the sensor, which is a standard manufacturing process of integrated microelectronic circuits. Figure4.2.2a shows the finished chip, and figure 4.2.2b how and where it is integrated into the probe This allows to obtain devices with a high signal-to-noise ratio. For the characterization of the prototypes, an electronic interface with discrete components was used and the two heaters were connected in a Wheatstone bridge configuration, as schematically shown in Figure 4.2.1(c). The output voltage of the bridge undergoes a high pass filter (CF, RF) that is amplified by an instrumentation amplifier (AD620) to eliminate the continuous component (see fig 4.2.2b) .

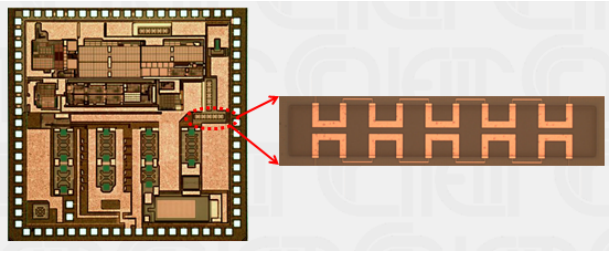

(a) Chip of the SIHT probe of the velocity transducer.

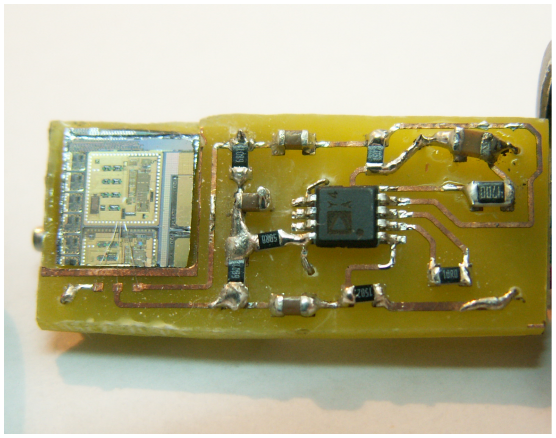

(b) SIHT velocity interface.

Figure 4.2.2: The SIHT probe, velocity interface.

4.2.2 Comparison Calibration of PV Probes

The new types of probes presented before could be used in many areas, and the laboratory of Ferrara (Italy) is collaborating with some realities that operate in different fields: medical [14], industrial, transport, pharmaceutical [15], musical [16]. The possibility to rely on these sensors has a number of positives outcomes, for example in terms of their innovative function and of the low cost of the probe itself.

The work that has been done for this dissertation will serve as a starting point for a possible future work related to the definition of a comparison calibration procedure for p-v probes. By considering the formula 3.3.5 it can be generalized as the formula below:

$$\Gamma(\omega) = \frac{Z_m}{Z_M}$$

where Z_m is the impedance measured by the SIHT probe under calibration and Z_M is the impedance measured by the reference probe, the Microflown® one, which has already been calibrated through the Matlab routine used in this dissertation. It can be easily seen that in a general field the characteristic impedance of a plane progressive wave, $\rho_0 c$, has been replaced with the Z_M term, which is be the reference function in a generalized field.

Acknowledgments

This dissertation has been made possible thanks to the contribution of the Institute of Italian National Research Council CNR- IDASC and the Deltatech in Sogliano al Rubicone (FC, Italy).

First of all I would like to thank Prof. Domenico Stanzial, who has been my professor for all these years and helped me with the work I have done in the laboratory.

Thanks to Prof. Romano Zannoli, for agreeing to be my referees, for its advices, patience and availability.

Thanks to Davide Bonsi for the advices, to be the one who give me the information to participate to a call for a four month grant in 2014 organized by the Consortium Spinner, hosted by the industry Deltatech, and allowed me to won one of the grants.

Thanks to IEIIT of Pisa for developing the probe, and in particular to Prof. Massimo Piotto for his constant availability, his patience and for his precious help.

Thanks to Gianni Fondriest, Ivan Fondriest of Deltatech, the municipality of Sogliano al Rubicone, the mayor Quintino Sabattini and the assessor Loredana Zamagni for the precious contribution to the project. I would like to thank Deltatech also to be my reference industry for the four month grant I won.

Appendix A - Matlab Code

Code to Calibrate the Pressure Sensitivity at 1000 Hz

```
function [sensitivity, Bruel_Sp, Fs] = Sensitivity_1000()
%output:
    %sensitivity - the values of sensitivity at 1000 Hz for pressure and
    %velocity of the Microflown probe
    %Bruel_Sp    - the sensitivity value for the Bruel probe
    %Fs          - sampling frequency

files = {'1000-bruel-8tac.wav','1000-mF-8can.wav'}; %reference audio files
Num = length(files);

for n = 1:Num
    [data,Fs,~,info]=wavread(files{n});
    if findstr(info.info.tras,'BK')~=0


        Bruel.info = info.info;
        Bruel.data = data(:,1);
        %S4C files normalized, it is needed to multiply them for
        %the maxr to obtain the effective value

        Bruel.maxr = str2num(Bruel.info.maxr);
        Bruel.fmax = str2num(Bruel.info.fmax);
        Bruel.fmin = str2num(Bruel.info.fmin);

    elseif findstr(info.info.tras, 'Microflown')~=0
        %         if j == 1
        mF.info = info.info;
        mF.P.data = data(:,1);
        mF.V.data = data(:,2);
        mF.fmax = str2num(mF.info.fmax);
        mF.fmin = str2num(mF.info.fmin);

    else
        error('error')
    end
end

NFFT =2^nextpow2(Fs);
Bruel.data = Bruel.data*Bruel.maxr;

mF.P.data = mF.P.data*str2num(mF.info.maxr);
Bruel.RMS = rms(Bruel.data);
mF.P.RMS = rms(mF.P.data);
mF.V.data = mF.V.data*str2num(mF.info.maxr);
mF.V.RMS = rms(mF.V.data);
% mF.V.RMS = rms(mF.V.data);

%Reference frequency founded in Larix with the ARTA software (a mean value
%over different measurements)
dB1000 =  88.1650;

Prif=20*(10^-6)*10^(dB1000/20); %Pressure value at 1000 Hz

Bruel_Sp = Bruel.RMS/(Prif); %sensitivity in V/Pa
sensitivity.P_Sp = mF.P.RMS/(Prif);
end
```

Code to Obtain the Gamma Correction curve

```
function [gamma,mF] = Gamma ()
%output:
    %gamma - amplitude and phase of the gamma function
    %mF    - all the necessary info taken from the audio files analysed

files = {'sweep-bruel1-8can.wav','sweep-mF1-8can'}; %Log sweep

Num = length(files);
for n = 1:Num
    [data,Fs,~,info]=wavread(files{n});
    if findstr(info.info.tras,'BK')~=0

        Bruel.info = info.info;
        Bruel.data = data(:,1);
        Bruel.fmax = str2num(Bruel.info.fmax);
        Bruel.fmin = str2num(Bruel.info.fmin);

    elseif findstr(info.info.tras, 'Microflown')~=0

        mF.info = info.info;
        mF.P.data = data(:,1);
        mF.V.data = data(:,2);
        mF.fmax = str2num(mF.info.fmax);
        mF.fmin = str2num(mF.info.fmin);

    else
        error('error')
    end

end

NFFT =2^nextpow2(Fs); f =Fs/2*linspace(0,1,NFFT/2+1);

rho = (101000*0.029)/(8.314*(273.15+18.5));%1.225 at 15°; %air density
c = 331.45 + 0.62*18.5; % sound velocity
       %derived from the first two terms of the Taylor expansion
I_0 = rho*c;

mF.P.data = mF.P.data*str2num(mF.info.maxr);
mF.V.data = mF.V.data*str2num(mF.info.maxr);

gamma.fft=tfestimate(mF.P.data,mF.V.data,hanning(NFFT/75),[],NFFT, Fs);
gamma.fft = 1./(gamma.fft*I_0);

gamma.dBA = 10*log(2*abs(gamma.fft(1:NFFT/2+1))); %sometimes the log to
%obtain dB is multiplied just for 10, the important is that every dB value
%has the same coefficient
gamma_Ph = angle(gamma.fft(1:NFFT/2+1));
gamma.Ph = gamma_Ph*180/pi;

[gamma.dBA,fi]=ottave(32,gamma.dBA,f);
subplot(1,2,1)
semilogx(fi, gamma.dBA);
xlim([50,8000])
xlabel('Frequency (Hz)'); ylabel('(dB)')
grid on
title('Amplitude')
subplot(1,2,2)
semilogx(f,gamma.Ph);
xlim([50,8000]); ylim([-175,175])
xlabel('Frequency (Hz)'); ylabel('(°)')
grid on
title('Phase')
```

Amplitude and phase of the velocity sensor

Code used to calculate the Sensitivity of the velocity sensor.

```
function [sensitivity, mF, gamma, f, S_f] = Sensitivity_V()
%output:
    %sensitivity - the values of sensitivity at 250 and 1000 Hz for
    %               pressure and velocity of the Microflown probe
    %mF          - all the necessary info taken from the audio files
    %               analysed updated with the new information
    %gamma       - amplitude and phase of the gamma function
    %f           - array of frequencies

sensitivity = Sensitivity_1000(); %sensitivity obtained at 1000 Hz
[gamma, mF] = Gamma (); %gamma function

files = uigetfile('.wav'); %I need just the microflown file and it's the
%user who choose which is the right file
Num = length(files);

[data,Fs,~,info]=wavread(files);
if findstr(info.info.tras, 'Microflown')~=0

    mF.info = info.info;
    mF.P.data = data(:,1);
    mF.V.data = data(:,2);
    mF.maxr = str2num(info.info.maxr);

else
    error('error')
end

NFFT =2^nextpow2(Fs); %number of samples, the Foruier transform work better
%with number of samples proportional to a power of two
f =Fs/2*linspace(0,1,NFFT/2+1); %frequencies

%to find the value of gamma at 250 Hz I preferred to use the value of the
%relative band of the one third octave spectrum
[gamma.terze,freq_eff]= ottave(3,gamma.fft,f);

[~,I] = min(abs(f-250));

%correction curve for the pressure microphone
S_f = 0.037.*(sqrt(1+(f./16946).^2))./(sqrt(1+(32./f).^2).*sqrt(1+(44./f).^2));

sensitivity.V250 = S_f(I)/sqrt(2)/abs(gamma.fft(I)); %[V/Pa]
end
```

Curves for the Amplitude and Phase of the VT transducer

Code autogenerated by Matlab® through the cftool application and used to calculate the corrected parameters of the amplitude and phase curves given by the constructor.

Below the code to obtain the calibrated curve for the correction of the velocity amplitude.

```
function [fitresult, gof] = V_Amp_cF(f, S, sens)
%CREATEFIT(F,S,SMF)
%  Create a fit.
%
%  Data for 'untitled fit 1' fit:
%      X Input : f
%      Y Output: S

%  Output:
%      fitresult : a fit object representing the fit.
%      gof : structure with goodness-of fit info.
%
%  See also FIT, CFIT, SFIT.

%  Auto-generated by MATLAB on 09-Mar-2016 22:09:03

%% Fit: 'untitled fit 1'.
[xData, yData] = prepareCurveData( f, S );

% Set up fittype and options.
Equation = strcat(num2str(sens),'/(sqrt(1+(a/x)^2)*(sqrt(1+(x/b)^2)*sqrt(1+(x/c)^2))*sqrt(1+(d/x)^2))');

ft = fittype( Equation, 'independent', 'x', 'dependent', 'y' );
opts = fitoptions( ft );
opts.Algorithm = 'Trust-Region';
opts.Display = 'Off';
opts.Lower = [0 0 0 0];
opts.MaxFunEvals = 1000;
opts.MaxIter = 100000;
opts.Robust = 'Bisquare';
opts.StartPoint = [0.546881519204984 0.957506835434298 0.964888535199277 0.157613081677548];
opts.Upper = [Inf Inf Inf Inf];

% Fit model to data.
[fitresult, gof] = fit( xData, yData, ft, opts );

% Plot fit with data.
figure( 'Name', 'untitled fit 1' );
h = plot( fitresult, xData, yData );

legend( h, 'S vs. f', 'untitled fit 1',  'Location', 'NorthEast' );
% Label axes
xlabel( 'f' );
ylabel( 'S' );
grid on
```

Below the code to obtain the VT correction curve for the phase.

```
function [fitresult, gof] = V_Ph_cF(Fp, Pgp)
%CREATEFIT(FP,PGP,VP)
%  Create a fit.
%
%  Data for 'untitled fit 1' fit:
%      X Input : Fp
%      Y Output: Pgp

%  Output:
%      fitresult : a fit object representing the fit.
%      gof : structure with goodness-of fit info.
%
%  See also FIT, CFIT, SFIT.

%  Auto-generated by MATLAB on 09-Mar-2016 22:28:28

%% Fit: 'untitled fit 1'.
[xData, yData] = prepareCurveData( Fp, Pgp );

% Set up fittype and options.
ft = fittype( '(-atan(a/x)+atan(x/b)+atan(x/c)-atan(d/x))/pi*180', 'independent', 'x',↙
'dependent', 'y' );
opts = fitoptions( ft );
opts.Algorithm = 'Trust-Region';
opts.Display = 'Off';
opts.Lower = [0 0 0 0];
opts.MaxFunEvals = 1000;
opts.MaxIter = 100000;
opts.Robust = 'Bisquare';
opts.StartPoint = [0.27692298496089 0.0461713906311539 0.0971317812358475 0.823457828327293];
opts.Upper = [Inf Inf Inf Inf];

% Fit model to data.
[fitresult, gof] = fit( xData, yData, ft, opts );

% Plot fit with data.
figure( 'Name', 'untitled fit 1' );
h = plot( fitresult, xData, yData );

legend( h, 'Pgp vs. Fp', 'untitled fit 1', 'Location', 'NorthEast' );
% Label axes
xlabel( 'Fp' );
ylabel( 'Pgp' );
grid on
```

Main Script

Matlab® function to find the corner frequencies through the best fit of the data.

```
%% Script to obtain the parameters of the calibration curves and the respectives graphs
clear all

[sensitivity, mF, gamma, f, S_f] = Sensitivity_V();
Fc =[142 573 4281 1]; %Microflown parameters
sensitivity.mF = 12.5./(sqrt(1+(Fc(1)./f).^2).*(sqrt(1+(f./Fc(2)).^2).*sqrt(1+(f./Fc(3)).^2)).*sqrt(1+(Fc(4)./f).^2)); %in V/m/s

sensitivity.vel = S_f'./(sqrt(2)*abs(gamma.fft)); %sensitivity of velocity through the gamma

[~,C_sup]=min(abs(f-10000));

[sensVott,f_ott]=ottave(32,sensitivity.vel(1:C_sup),f(1:C_sup));

[CF_V, gof] = V_Amp_cF(f_ott, sensVott, sensitivity.V250); %function obtained through
                        %the cftool %sensmFott
sensitivity.calc = CF_V(f); %sensitivity obtained through the parameters of
                        %the curve fitting
NFFT =2^nextpow2(48000);

%% Calcultion of the calibrated velocity and plot of the curves

V.mF = (1./sensitivity.mF); %in  m/s/V
V.gamma = (1./sensitivity.vel);
V.mio = (1./sensitivity.calc);

V.mF_dB = 10*log(V.mF(1:NFFT/2+1)); %dB
V.gamma_dB = 10*log(V.gamma(1:NFFT/2+1));
V.mio_dB = 10*log(V.mio(1:NFFT/2+1));
free =f;
[V.mF_dB]=ottave(32,V.mF_dB(1:C_sup),f(1:C_sup));
[V.gamma_dB]=ottave(32,V.gamma_dB(1:C_sup),f(1:C_sup));
[V.mio_dB,f]=ottave(32,V.mio_dB(1:C_sup),f(1:C_sup));

figure('Name','Magnitude correction of the VT','NumberTitle','off')
semilogx(f, V.mF_dB,'b', f, V.mio_dB, 'r', f, V.gamma_dB, 'g')
legend('Nominal curve','Analytical curve best fit','Experimental curve')
xlim([50 10000])
ylim([-30 20])
grid on
xlabel('Frequency [Hz]')
ylabel('Amplitude [dB]')
title('Magnitude correction of the VT')

%% Calculation of the calibrated phase and plot of the results obtained

f = free;
V_Phase_mF = (-atan(113./f)+atan(f./625)+atan(f./8030)-atan(1./f))/pi*180; %Phase correction in degree
P_Phase = (atan(37./f)+atan(32./f)+atan(f./50865));
[~,C_sup]=min(abs(f-10000));
Pg =(angle(gamma.fft)-P_Phase')/pi*180 ;%degree

[CF_V_Ph, gof] = V_Ph_cF(f(1:C_sup), Pg(1:C_sup));%,V_Phase_mF(1:C_sup));
Ph_calib = CF_V_Ph(f); %

[~,C_sup]=min(abs(f-10000));
figure('Name','Phase correction of the VT','NumberTitle','off')
semilogx( f(1:C_sup), V_Phase_mF(1:C_sup), 'b',  f(1:C_sup), Ph_calib(1:C_sup),'r',f(1:C_sup), Pg(1:C_sup),'g')
legend('Nominal curve',  'Analytical curve best fit', 'Experimental curve')
xlim([50 10000])
ylim([-150 150])
grid on
xlabel('Frequency [Hz]')
ylabel('Phase [deg]')
title('Phase correction of the VT')
```

Appendix B - Octave Bands Division

Below the code used to divide the audio in octave bands using the relation defined in section 1.6

```
function [data,freq_eff]= ottave(frac, fileDati, frequenze)
%input:
    %frac      - fraction of the octave to analyze (1 = one octave band;
    %3 = one third octave band; etc)
    %fileDati  - file to divide in octave bands
    %frequenze - array of frequencies
%output:
    %data      - file divided in bands
    %freq_eff  - central frequency of the band

f = 1000; %reference frequency

n = 1;
f_inf(1) = f;
while f_inf(n) >= 1

    f_inf(n+1)=f_inf(n)/2^(1/frac);

    n = n+1;
end

n=1;

f_sup(1) = f;
while f_sup(n) <= 20000

    f_sup(n+1)=f_sup(n)*2^(1/frac);

    n = n+1;
end

f_inf = f_inf(length(f_inf):-1:2);
f_cent = [f_inf f_sup];

f_inf = f_cent./2^(1/(2*frac));
f_sup = f_cent.*2^(1/(2*frac));

for i=1:length(f_inf)
[~,InInf(i)] = min(abs(f_inf(i)-frequenze));
[~,InSup(i)] = min(abs(f_sup(i)-frequenze));
end

% fileDati=fileDati*10^4;

for i = 1:length(InInf)
    A = fileDati(InInf(i):InSup(i));

data(i) = mean(A);
end
freq_eff = f_cent;
```

Bibliography

[1] D. Stanzial, G. Sacchi, and G. Schiffrer. *Calibration of pressure-velocity probes using a progressive plane wave reference field and comparison with nominal filters.* J. Acoust. Soc. Am., (129): 3745–3755, 2011.

[2] W. C. Elmore, M. A. Heald., *The Physics of Waves*, McGraw-Hili, Inc., 1969.

[3] F. Jacobsen, *An elementary introduction to acoustics*, in Fundamentals of Acoustics and Noise Control, Note no 31200: 1-51, 2011.

[4] Brüel&Kjær, *Technical Documentation - Microphone Handbook*, Volume 1: Theory, Brüel&Kjær®.

[5] Microflown, *Calibration Report - Microflown® Technologies probe*: PT0702-03, 17-04-2013.

[6] D. A. Bies and C. H. Hansen, *Engineering Noise Control - Theory and Practice*, 4th Edition, Spon Press, 2009.

[7] I. Mateljan, *ARTA User manual*, 2014.

[8] H. E. de Bree, *The Microflown® E-book*, 2007.

[9] F. Jacobsen, V. Jaud, *A note on the calibration of pressure-velocity sound intensity probes*, J. Acoust. Soc. Am. (120), 830-837, 2006.

[10] MathWorks, *Constrained Nonlinear Optimization Algorithms*, http://uk.mathworks.com/help/optim/ug/constrained-nonlinear-optimization-algorithms.html

[11] MathWorks, *Least-Squares Fitting*, http://it.mathworks.com/help/curvefit/least-squares-fitting.html

[12] F. Fimiani, D. Bonsi, P. Bruschi, M. Buiat, M. Piotto, and D. Stanzial. *Calibrazione per confronto delle sonde pressione-velocità (p-v): impostazione del problema*, in Proceedings of 41° National Conference AIA, Pisa, Italia, June 2014.

[13] Bruschi, P., Butti, F., Piotto, M., *CMOS Compatible Acoustic Particle Velocity Sensors*, Proceedings of IEEE Sensors 2011, Limerick (Ireland) 28-31 October 2011, pp. 1405-1408.

[14] F. Fimiani, *Confronto di dati timpanometrici ottenuti con strumentazione standard e con sonde pressione-velocità*, Thesis, 2012

[15] M. Buiat, *Comparison Calibration of Low-Cost Prototypes of Acoustic Pressure-Velocity Probes and Some Application Case-Studies*. Ph.D. Thesis, 2014.

[16] F. Fimiani, M. Buiat, D. Bonsi, D. Stanzial, *Scanning a flue organ pipe with a p-v probe*, in Proceedings of Forum Acusticum 2015, Krakow, Poland, September 2015.